5-20-2011

Collapse Transition of Randomly Branched Polymers: Renormalized Field Theory

Hans-Karl Janssen
Institut für Theoretische Physik III

Olaf Stenull
University of Pennsylvania, stenull@sas.upenn.edu

Suggested Citation:
Janssen, H. and Stenull, O. (2011). Collapse transition of randomly branched polymers: Renormalized field theory. *Physical Review E.* **83**, 051126.

http://dx.doi.org/10.1103/PhysRevE.83.051126

Collapse Transition of Randomly Branched Polymers: Renormalized Field Theory

Abstract

We present a minimal dynamical model for randomly branched isotropic polymers, and we study this model in the framework of renormalized field theory. For the swollen phase, we show that our model provides a route to understand the well-established dimensional-reduction results from a different angle. For the collapse θ transition, we uncover a hidden Becchi-Rouet-Stora supersymmetry, signaling the sole relevance of tree configurations.We correct the long-standing one-loop results for the critical exponents, and we push these results on to two-loop order. For the collapse θ transition, we find a runaway of the renormalization group flow, which lends credence to the possibility that this transition is a fluctuation-induced first-order transition. Our dynamical model allows us to calculate for the first time the fractal dimension of the shortest path on randomly branched polymers in the swollen phase as well as at the collapse transition and related fractal dimensions.

Disciplines

Physical Sciences and Mathematics | Physics

Comments

Suggested Citation:

Janssen, H. and Stenull, O. (2011). Collapse transition of randomly branched polymers: Renormalized field theory. *Physical Review E.* **83**, 051126.

http://dx.doi.org/10.1103/PhysRevE.83.051126

Collapse transition of randomly branched polymers: Renormalized field theory

Hans-Karl Janssen
Institut für Theoretische Physik III, Heinrich-Heine-Universität, D-40225 Düsseldorf, Germany

Olaf Stenull
Department of Physics and Astronomy, University of Pennsylvania, Philadelphia, Pennsylvania 19104, USA
(Received 16 February 2011; published 20 May 2011)

We present a minimal dynamical model for randomly branched isotropic polymers, and we study this model in the framework of renormalized field theory. For the swollen phase, we show that our model provides a route to understand the well-established dimensional-reduction results from a different angle. For the collapse θ transition, we uncover a hidden Becchi-Rouet-Stora supersymmetry, signaling the sole relevance of tree configurations. We correct the long-standing one-loop results for the critical exponents, and we push these results on to two-loop order. For the collapse θ' transition, we find a runaway of the renormalization group flow, which lends credence to the possibility that this transition is a fluctuation-induced first-order transition. Our dynamical model allows us to calculate for the first time the fractal dimension of the shortest path on randomly branched polymers in the swollen phase as well as at the collapse transition and related fractal dimensions.

DOI: 10.1103/PhysRevE.83.051126 PACS number(s): 64.60.ae, 05.40.−a, 64.60.Ht

I. INTRODUCTION

Randomly branched polymers (RBPs) are a classical topic in statistical physics. Seminal advancements in the theoretical understanding of these polymers [1–5] have been made not long after the advent of renormalization group theory starting with the seminal work of Lubensky and Issacson (LI). With the surge of biophysics, there recently has been renewed interest in RBPs because RNA in its molten phase belongs to the same universality class as swollen RBPs [6,7]. However, the current understanding of RBPs is still not quite satisfactory. For example, the topology of their phase diagram is not entirely clear. In particular the part of the phase diagram that contains the so-called θ' transition gives reason for debate. The existing theories [1,2] for the collapse θ transition are not entirely correct. As far as we know, there exist no theories for the transport properties and the related fractal dimensions of RBPs such as the dimensions of the backbone, the shortest path, and so on.

In this paper we are not interested in chemical or mechanical properties of randomly branched polymers. Rather, we are interested in their structure. More precisely, we are interested in their universal structural properties in the limit where the number of constituent monomers is large. In this limit, an RBP can be regarded as a large cluster, and its structural properties are universal, i.e., common to large RBPs as a class irrespective of their physical or chemical details. Phenomenologically, only their large size and their branching on all length scales are relevant. In the language of critical phenomena—phenomena with large correlation lengths, here the diameters of clusters—all such systems of fractal clusters with different microscopic aspects but with these common relevant properties belong to one universality class, which we denote in the following with the *pars pro toto* randomly branched polymers. In computer simulations such clusters are usually constructed as so-called lattice animals, i.e., clusters of connected sites (monomers) on a d-dimensional regular lattice. The recent publication of Hsu and Grassberger on the collapse transition of animals [8] and the unresolved issues mentioned above have triggered us to reconsider this classical topic with field theoretic methods.

In the much-studied case of a single large linear polymer in a diluted solvent, the phase diagram is one-dimensional. When the solvent quality is lowered (typically by lowering its temperature) below the so-called θ point, the polymer undergoes a collapse transition from a swollen coillike conformation to a compact globule-like conformation. In simple lattice models, the monomer-solvent repulsion that drives the collapse transition is generically implemented via an effective attractive interaction between nonbonded monomers, which is equivalent to the monomer-solvent repulsion at least as far as universal properties are concerned. Thus, the fugacity for nonbonded monomer-monomer contacts, here called $z_{\rm cont}$, can be chosen as the control variable spanning the phase diagram of a linear polymer in a solvent. Evidently, $z_{\rm cont}$ is closely related to temperature.

In the case of a single large RBP in a diluted solvent, the phase diagram is two-dimensional; see Fig. 1. The basic reason for the additional dimension is that one has to deal with an additional fugacity stemming from the fact that the number of bonds b of an RBP is not uniquely determined by its number of sites N, $b - N + 1 =: l \geqslant 0$, whereas it is uniquely determined for a linear polymer (as well as for a treelike branched polymer) with $l = 0$. The additional fugacity, here called $z_{\rm cycle}$, regulates the cyclomatic index (the number of cycles l) of the polymer in the grand partition sum. For $z_{\rm cycle} = 0$, the RBP has no cycles and the minimal number of bonds (i.e., it is treelike), and the phase diagram becomes one-dimensional (it reduces to the vertical axis with $z_{\rm cycle} = 0$ in Fig. 1). Physically, $z_{\rm cycle}$ can be varied, e.g., by adding polyfunctional chemical units to the solution whose insertion into RBP results in additional bond cycles.

Over the last two decades or so, a number of numerical studies have been undertaken to map out this phase diagram [8–14]. The picture that arises from these studies can be summarized as follows: There is a swollen phase where the polymer is in a treelike or spongelike conformation and a

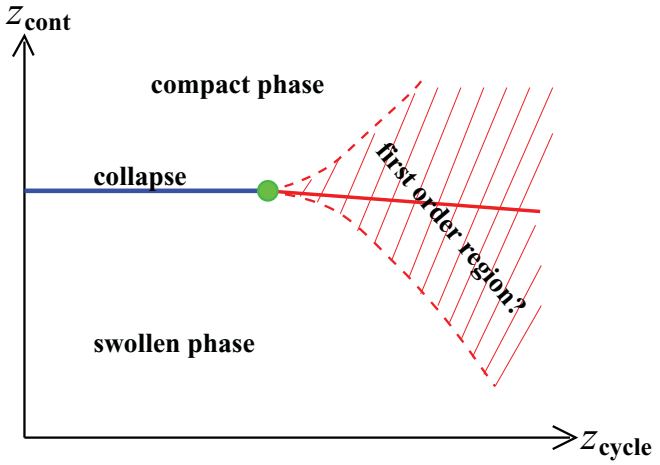

FIG. 1. (Color online) Schematic phase diagram for an RBP modeled by a lattice animal in the limit of a large number of constituents. z_{cont} is the fugacity for contacts between nonbonded monomers, and z_{cycle} is the fugacity for closed monomer cycles on the polymer.

compact phase where the polymer is in a coillike or vesicle-like conformation. There is some debate whether there exists a phase transition between the two compact conformations or not. Between the swollen and the compact phases, there is a line of collapse transitions. One part, called the θ line (labeled collapse, blue), corresponds to continuous transitions with universal critical exponents from the treelike conformation to the coillike confirmation. The other part of the transition line, called the θ' line (red, in the dashed region), corresponds to the transition between the foam- or spongelike conformation to the vesicle-like conformation. Between the θ and θ' lines there is a tricritical point. There has been some controversy if the θ' transition is continuous or not. With the assumption of it being continuous, computer simulations in two dimensions yield nonuniversal critical exponents [8]. As we will explain in detail below, our renormalization group (RG) study shows that the collapse transition to the right of the tricritical point is characterized by a runaway of the RG flow. This suggests that the θ' transition is a fluctuation-induced first-order transition instead. It could also mean that two of the lines observed in numerical studies of the phase diagram, *namely,* the lines interpreted as the line of transitions between two compact phases and the θ' line, respectively, are merely shadows of the spinodals of the discontinuous transition.

The most fruitful theoretical approach to RBPs is based on the asymmetric Potts model [1,3,15], although Flory theory [2] and real space renormalization [16] have also been applied successfully. For the swollen phase, the field theoretic problem was settled by Parisi and Sourlas (PS) via mapping the relevant part of the asymmetric Potts model to the Yang-Lee edge problem using dimensional reduction [4]. Subsequently, this mapping has been applied to further problems such as the exact calculation of universal scaling functions characterizing the behavior in the physical dimension 3 [17–19]. Dimensional reduction was confirmed later with the discovery of an exact relationship between swollen RBP models and repulsive gases at negative activity in two fewer dimensions by Brydges and Imbrie [20,21].

The asymmetric Potts model also provides a vantage point for studying the θ transition and is the basis of the seminal field theoretic work of LI [1] and Harris and Lubensky [3]. Their one-loop calculation for the θ transition, however, contains a systematic error in the RG procedure, and as a consequence their long-standing one-loop results for the collapse transition are strictly speaking not correct, although the numerical deviation from the correct results is fortunately small.

Very recently we developed a new dynamical field theory for RBPs; see Ref. [22] for a brief account. In the present paper, we extend our work, and we present it in more detail to make it easier accessible for nonspecialist readers. Our theory is based on a stochastic epidemic process that models especially dynamical percolation with a tricritical instability [23]. As we will discuss in detail below, we focus entirely on the the nonpercolating phase of the process. There, the very large clusters that finally result have the same statistics as RBPs [24]. The tricritical instability of the process, in particular, gives us a handle on the statistics of collapsing RBPs. We discuss the relation of our model to the asymmetric Potts model and carefully analyze its symmetries. In the swollen phase, the model has a high supersymmetry including translation and rotation invariance in superspace and leads to the well-known Parisi-Sourlas dimensional reduction [4]. At the collapse transition, superrotation symmetry is lost, and only translation invariance in superspace, i.e., Becchi-Rouet-Stora (BRS) symmetry [25], is restituted at the fixed point of the renormalization group. The appearance of BRS symmetry shows that only treelike RBPs [5,21] are relevant also at the collapse transition. We perform a two-loop renormalization group (RG) calculation, which corrects and extends the long-standing LI results for the collapse transition. Furthermore, we show that the θ' transition is characterized by a runaway of the RG flow, which suggests that this transition is a fluctuation-induced first-order transition contrary to what has been assumed in recent numerical studies [8–14].

The outline of our paper is as follows: In Sec. II, we derive our dynamical field theoretical model starting from the Langevin equation for a generalization of the so-called general epidemic process (GEP). We discuss different limits of this model and recast it into different forms to reveal the symmetry contents and to establish the connections to previous work in particular that of LI and PS. In Sec. III we present the core of our RG analysis with focus on the θ transition. We define our RG scheme, and we set up RG equations. We analyze the RG flow and its fixed points, and we point out the implication of this flow for the θ' transition. In Sec. IV, we extract from our RG results for various observables common in polymer physics. In particular, we calculate scaling forms and critical exponents for the θ transition. We also present results for the fractal dimension of the minimal path on RBPs at the collapse transition and in the swollen phase. At the collapse transition, in particular, this fractal dimension determines several other fractal properties since large RBPs are effectively treelike. In Sec. V, we give a few concluding remarks. There are three appendixes that present additional

information and some of the more technical aspects of our study.

II. MODELING RANDOMLY BRANCHED POLYMERS

In this section we develop our model for RBPs based on the GEP, which is perhaps the most widely studied reaction diffusion process in the universality class of dynamical isotropic percolation. To be more specific, we use a generalization of this process that allows for a tricritical instability. We will start with the Langevin equation for this generalized GEP, which we will refine into a minimal model in the sense of renormalized field theory. For background on field theory methods in general, we refer to Refs. [26,27]. For background on dynamical field theory in the context of percolation problems, we refer to Ref. [28]. For a related approach to the somewhat simpler problem of directed randomly branched polymers, see Ref. [29].

A. Lattice animals

Usually one models RBPs by means of so-called lattice animals, which are nothing but clusters of connected sites on a regular lattice. One considers as the primary quantity the number $\mathcal{A}(N,l,c)$ of all different configurations (up to translations) of a single cluster (animal), which is a collection of N sites, connected by $b \geqslant N-1$ bonds, l cycles of the bonds, and c contacts (nearest-neighbor pairs of nonbonded sites). The number of occupied bonds is then given by $b = l + N - 1$. There is no need for introducing a separate number s of nearest-neighbor pairs of occupied and nonoccupied sites. This number is given by the relation $\mathcal{N}N = 2b + 2c + s$, where $\mathcal{N}$ is the lattice coordination number, which is equal to $2d$ on a simple hypercubic lattice. The weighted animal number

$$\mathcal{A}_N(z_{cy},z_{co}) = \sum_{l,c} \mathcal{A}(N,l,c) z_{cy}^l z_{co}^c \tag{2.1}$$

represents a general partition sum for the system. If one sets z_{cy} to zero, the sum includes only tree configurations. It is well known that this partition function, also known as the generating function of lattice animals, can be obtained from the asymmetric $(n+1)$-state Potts model in the limit $n \to 0$ [1,3,15], and it is this connection that stands behind the seminal earlier results on RBPs; see Sec. I.

Typically one considers the partition sum for large animals: $N \gg 1$. The phase diagram in this limit in terms of the fugacities z_{cy} and z_{co} is shown in Fig. 1. The special curve $z_{cy} = (z_{co}-1)z_{co}$, parametrized by a bond probability p as $z_{cy} = p/(1-p)^2$, $z_{co} = 1/(1-p)$ defines a bond-percolation model with the critical percolation probability $p = p_c$ depending on the specific type of the lattice. In general, if $N \gg 1$, there is a swollen phase for small fugacities, and a compact phase separated by the collapse transition line $z_{co}(z_{cy})$, which consists of two parts separated by the percolation point as a higher-order critical point. Whereas in the swollen phase $\mathcal{A}_N(z_{cy},z_{co}) \sim \kappa_{sw}(z_{cy},z_{co})^N N^{-\dot\theta}$ with universal $\dot\theta$ and nonuniversal $\kappa_{sw}(z_{cy},z_{co})$, one finds at least for the left part of the transition line the scaling law

$$\mathcal{A}_N[z_{cy},z_{co}(z_{cy})] \sim \kappa(z_{cy})^N N^{-\theta} \tag{2.2}$$

with nonuniversal $\kappa(z_{cy})$ and universal θ in general different from $\dot\theta$ [8]. The percolation point as a separating point on the transition line with higher-order critical behavior has a $\theta_{\rm perc}$ that is in general different from θ and $\dot\theta$. Only in mean-field theory (Landau approximation) these exponents are equal: $\theta = \dot\theta = \theta_{\rm perc} = 5/2$.

Other fundamental quantities are given by correlations of sites on the cluster. The correlation function may be defined by

$$G_N(\mathbf{r},\mathbf{r}') = \frac{1}{\mathcal{A}_N(z_{cy},z_{co})} \sum_{l,c} \mathcal{A}(N,l,c;\mathbf{r},\mathbf{r}') z_{cy}^l z_{co}^c, \tag{2.3}$$

where $\mathcal{A}(N,l,c;\mathbf{r},\mathbf{r}')$ is the total number of clusters with N sites, l loops, and c contacts, containing the lattice sites $\mathbf{r}$ and $\mathbf{r}'$. Of course, it is

$$\sum_{\mathbf{r}} \mathcal{A}(N,l,c;\mathbf{r},\mathbf{r}') = N\mathcal{A}(N,l,c). \tag{2.4}$$

The radius of gyration R_N is then defined by

$$R_N^2 = \frac{1}{2dN} \sum_{\mathbf{r},\mathbf{r}'} (\mathbf{r}-\mathbf{r}')^2 G_N(\mathbf{r},\mathbf{r}'). \tag{2.5}$$

For $N \gg 1$, it shows also an universal scaling law

$$R_N \sim N^{\nu_A}. \tag{2.6}$$

The fractal dimension $d_f = 1/\nu_A$ is different at the transition line from its value in the swollen phase and at the separating percolation point. However, in mean-field theory it has the uniform value $d_f = 4$. Of course, in the compact phase, the fractal dimension is always equal to the lattice dimension d.

B. Reactions, Langevin equation, and dynamic response functional

The model that we are about to develop is in the spirit of Landau's ideas for modeling second-order phase transitions; i.e., it is a mesoscopic model that focuses on general principles unifying processes belonging to the same universality class and is therefore necessarily phenomenological [28]. To set the stage, however, we find it worthwhile to discuss in some detail a specific model belonging to the RBP universality class, namely, a generalization of the GEP. The reaction-diffusion equations defining this process will nurture our intuition and will help us to establish our ideas.

The following generalization of the GEP is a variant of a process that we have introduced for the description of tricritical isotropic percolation [23]. We denote by $X(\mathbf{r})$ an agent, i.e., an infected individual, at site $\mathbf{r}$. An agent can infect a neighboring site $\mathbf{r}+\delta$ via the percolation step

$$X(\mathbf{r}) \to X(\mathbf{r}) + X(\mathbf{r}+\delta). \tag{2.7}$$

This fundamental reaction gives rise to spreading and branching of the epidemic. The agents can spontaneously become immune (or decay) and produce spam as a marker of the agent through the reactions

$$X(\mathbf{r}) \to Z(\mathbf{r}), \tag{2.8a}$$

$$X(\mathbf{r}) \to X(\mathbf{r}) + Z(\mathbf{r}), \tag{2.8b}$$

where $Z(\mathbf{r})$ denotes an immune individual or spam at site $\mathbf{r}$. In the language of forest fires, $Z(\mathbf{r})$ are also referred to as debris. It is the debris left behind by the epidemic that forms the clusters that serve us as prototypes for RBPs. Their self-avoidance or excluded volume interaction is modeled with help of the reaction

$$X(\mathbf{r}) + kZ(\mathbf{r}) \to (k+1)Z(\mathbf{r}), \tag{2.9}$$

where $k = 1,2,\ldots$, which dampens the epidemic. A mechanism for the RBPs to compactify is introduced into the process through the reaction

$$X(\mathbf{r}-\delta) + Z(\mathbf{r}+\delta) \to X(\mathbf{r}-\delta) + X(\mathbf{r}) + Z(\mathbf{r}+\delta), \tag{2.10}$$

which simulates an effective attraction of the agents by the debris.

Having these reactions, one possible way to proceed would be to reformulate the corresponding master equation in terms of bosonic creation and annihilation operators and then to produce a field theoretic action from these operators via coherent state path integrals [30]. However, we prefer to extract directly the mesoscopic Langevin equations that incorporate the universal features of the above reactions, namely, the percolation of agents, their spontaneous decay, their suppression and possible effective attraction by the debris, and the possible existence of vacua without agents as absorbing states of the system.

The primary density fields describing our generalized GEP are the field of agents $n(\mathbf{r},t)$ and the field of the inactive debris $m(\mathbf{r},t) = \lambda \int_{-\infty}^{t} dt'\, n(\mathbf{r},t')$, which ultimately forms the polymer cluster. A non-Markovian Langevin equation describing such a process, and representing therefore the universality class, is given by

$$\lambda^{-1}\partial_t n = \nabla^2 n + c\nabla m\cdot\nabla n - \left(r + g'm + \frac{f'}{2}m^2\right)n + \zeta. \tag{2.11}$$

Here the parameter r tunes the "distance" to the percolation threshold. Below this threshold, i.e., in the absorbing phase, r is positive. Throughout this paper, we will assume that the system is deep in the absorbing phase. In this case a typical final cluster generated from an additional source $q\delta(\mathbf{r})\delta(t)$ of agents (adding such a source is equivalent to specifying an initial condition for the process) consists of $N = \langle \int d^d r\, m(\mathbf{r},\infty)\rangle \approx q/r$ debris particles and has a mean diameter $1/\sqrt{r}$. However, we are interested in the large nontypical clusters, the rare events of the stochastic process, with $N \gg q/r$. We know from percolation theory [24] that these clusters belong to the universality class of lattice animals. Hence, they are the same in a statistical sense as randomly branched polymers as far as their universal properties go. The gradient-term proportional to c describes the attractive influence of the debris on the agents if c is negative (as a negative contribution to g' does). At this point other forms of gradient terms such as $m\nabla^2 n$ and $n\nabla^2 m$ are conceivable. However, as long as we include any one of these gradient terms into our theory, an omission of the other gradient terms has no effect on the final results, and we choose to work with the term proportional to c only for simplicity. For usual percolation problems (ordinary or tricritical), these gradient terms are irrelevant. As long as $g' > 0$, the second-order term $f'm^2$ is irrelevant near the transition point, and the process models ordinary percolation near $r = 0$ [31] or nontypical very large clusters, the swollen RBPs, for $r > 0$. We permit both signs of g' (negative values of g' correspond to an attraction of the agents by the debris; see above). Hence, our model allows for a tricritical instability (tricritical percolation near $r = 0$ [23] or the collapse transition of the RBPs for $r > 0$). Consequently we need the second-order term $f' > 0$ (which represents the self-avoidance property) to limit the density to finite values. Physically it originates from the suppression of agents by the debris. The Gaussian noise source $\zeta(\mathbf{r},t)$ has correlations

$$\overline{\zeta(\mathbf{r},t)\zeta(\mathbf{r}',t')} = [\lambda^{-1}gn(\mathbf{r},t)\delta(t-t') - fn(\mathbf{r},t)n(\mathbf{r}',t')]\delta(\mathbf{r}-\mathbf{r}'). \tag{2.12}$$

The process is assumed to be locally absorbing, and thus all terms in the noise-correlation function contain at least one power of n. The first part of the noise correlation takes into account that the agents decay spontaneously, and thus $g > 0$. The non-Markovian term proportional to f simulates the anticorrelating or, respectively, correlating (from attraction) behavior of the noise in regions where debris has already been produced, with f being negative if the attraction effects are overwhelming.

Two points are worth mentioning at this stage: (1) For the Langevin equation with the local noise to be meaningful mathematically, an appropriate cutoff procedure of long wavelengths has to be used. (2) The stochastic process (2.11) with $c = r = g' = f' = g = 0$ but $f > 0$ belongs to the universality class of self-avoiding random walks (SAW) and generates therefore the statistics of linear polymers [32].

To proceed toward a field theoretic model, the Langevin equations are now transformed into a stochastic response functional in the Itô sense [28,33–35]:

$$\mathcal{J} = \int d^d x\left[\lambda\int dt\tilde{n}\left(\lambda^{-1}\partial_t - \nabla^2 - c\nabla m\cdot\nabla + r + g'm + \frac{f'}{2}m^2 - \frac{g}{2}\tilde{n}\right)n + \frac{f}{2}\left(\lambda\int dt\,\tilde{n}n\right)^2\right]. \tag{2.13}$$

With this functional, we now have a vantage point for the calculation of statistical quantities via path integrals with the exponential weight $\exp(-\mathcal{J})$. When a source term $(\tilde{h},\tilde{n})$ is added, where $\tilde{h}(\mathbf{r},t) = \tilde{h}_0(\mathbf{r},t) = q\delta(\mathbf{r})\delta(t)$ and $(..,..)$ denotes an integral of a product of two fields over space and time, this functional describes, in particular, the statistics of clusters of debris generated by the stochastic process (2.11) from a source of q agents at the point $\mathbf{r} = 0$ at time zero. Denoting by Tr[...] the functional integration over the fields, we generally have

$$\mathrm{Tr}[\exp(-\mathcal{J} + (\tilde{h},\tilde{n}) + (h,n)] = 1 \tag{2.14}$$

if h *or* $\tilde{h}$ is zero. The first property follows from causality, whereas the second originates from the absorptive properties of the process. Note that the role of causality and adsorptivity can be interchanged via the duality transformation $m(\mathbf{r},t) \longleftrightarrow -\tilde{n}(\mathbf{r},-t)$ [28,31,36].

C. Branched polymers as rare events

Averaging an observable $\mathcal{O}[n]$ over final clusters of debris (the RBPs) of a given mass N generated from a source $\tilde{h}(\mathbf{r},t) = q\delta(\mathbf{r})\delta(t)$ of agents at the origin $\mathbf{r} = 0$ at time $t = 0$ leads to the quantity [28,31,36]

$$\begin{aligned}\langle\mathcal{O}\rangle_N\mathcal{P}(N) &= \langle\mathcal{O}[n]\delta(N-\mathcal{M})\exp[(\tilde{h},\tilde{n})]\rangle \\ &= \mathrm{Tr}[\{\mathcal{O}[n]\delta(N-\mathcal{M})\exp[-\mathcal{J}+q\tilde{n}(0,0)]\} \\ &\simeq q\,\mathrm{Tr}[\mathcal{O}[n]\tilde{n}(0,0)\delta(N-\mathcal{M})\exp(-\mathcal{J})], \quad (2.15)\end{aligned}$$

where

$$\mathcal{P}(N) = \langle\delta(N-\mathcal{M})\exp[q\tilde{n}(0,0)]\rangle \quad (2.16)$$

is the probability distribution for finding a cluster of mass N, and

$$\mathcal{M} = \int d^d r dt\, \lambda n(\mathbf{r},t) = \int d^d r\, m_\infty(\mathbf{r}) \quad (2.17)$$

is the total mass of the debris. The field $m_\infty(\mathbf{r}) = m(\mathbf{r},t=\infty)$ describes the distribution of the debris after the epidemic has become extinct. Since the probability distribution should be proportional to the number of different configurations, we expect by virtue of universality arguments the following proportionality between the probability distribution $\mathcal{P}(N)$ and the lattice animal number $\mathcal{A}_N$ for asymptotically large N:

$$\mathcal{A}_N \sim N^{-1}\kappa_0^N\mathcal{P}(N), \quad (2.18)$$

where κ_0 is an effective coordination number of the underlying lattice. The fugacities in $\mathcal{A}_N(z_{cy},z_{co})$ are then considered as analytical functions of the different parameters in the response functional $\mathcal{J}$ or vice versa. The factor N^{-1} arises in Eq. (2.18) because the generated clusters are rooted at the source at the point $\mathbf{r} = 0$, and each site of a given lattice animal may be the root of given cluster. Hence, we expect a scaling

$$\mathcal{P}(N) \sim N^{1-\theta}p_0^N \quad (2.19)$$

with an universal scaling exponent θ but nonuniversal p_0.

In actual calculations, the delta function appearing in averages like in Eq. (2.16) is hard to handle. This problem can be simplified by using Laplace-transformed observables like, e.g., the Laplace transformation of $\mathcal{P}(N)$, which are functions of a variable conjugate to N, e.g., z,

$$\mathcal{P}(N) = \int_{\sigma-i\infty}^{\sigma+i\infty}\frac{dz}{2\pi i}\,\mathrm{e}^{zN}\,\langle\exp[-z\mathcal{M}+q\tilde{n}(0,0)]\rangle, \quad (2.20)$$

and applying inverse Laplace transformation (where all the singularities of the integrand lie to the left of the integration path) in the end. Note that the relationship between $\mathcal{P}(N)$ and $\mathcal{A}_N$ signals the existence of a singularity $\sim(z-z_c)^{\theta-2}$ of the integrand in Eq. (2.20) at some critical value z_c. The switch to Laplace-transformed observables can be done in a pragmatic way by augmenting the original $\mathcal{J}$ with a term $z\mathcal{M}$ and then working with the new response functional

$$\mathcal{J}_z = \mathcal{J} + z\mathcal{M}. \quad (2.21)$$

Denoting averages with respect to the new functional by $\langle\ldots\rangle_z$, and defining

$$q\,\Phi(z) = \ln\langle\exp(q\tilde{n})\rangle_z \approx q\,\langle\tilde{n}\rangle_z \quad (2.22)$$

for small q, we get by using Jordan's lemma that the asymptotic behavior for large N is given by

$$\begin{aligned}\mathcal{P}(N) &= \int_{\sigma-i\infty}^{\sigma+i\infty}\frac{dz}{2\pi i}\,\exp[zN+q\,\Phi(z)] \\ &= \mathrm{e}^{z_cN+q\Phi(z_c)}\int\frac{dz'}{2\pi i}\,\exp\{z'N \\ &\quad + q[\Phi(z_c+z')-\Phi(z_c)]+O(q^2)\} \\ &\approx q\mathrm{e}^{z_cN+q\Phi(z_c)}\int_0^\infty dx\,\frac{\mathrm{Disc}\Phi(z_c-x)}{2\pi i}\mathrm{e}^{-xN}, \quad (2.23)\end{aligned}$$

where the last row gives the asymptotics for large N and small q. Here z_c is the first singularity of $\Phi(z)$, which as we will show is a branch point on the negative real axis, and the contour of the path integral is deformed into a path above and below the branch cut beginning at the singularity. DiscΦ denotes the discontinuity of the function Φ at the branch cut. The nonuniversal factor $q\mathrm{e}^{z_cN+q\Phi(z_c)}$ depending exponentially on N is common to all averages defined by Eq. (2.15) and therefore cancels from all mean values $\langle\mathcal{O}\rangle_N$.

D. Mean-field theory

Before we assend to the heights of field theory (or descend to its depths, if the reader prefers), we first apply a mean-field approximation to our theory; i.e., we solve the functional integrals with the weight $\exp(-\mathcal{J}_z)$ using a saddle-point approximation. The linear term in $\mathcal{J}_z$ that is proportional to the Laplace variable z leads to a nonzero saddle-point value of the field $\tilde{n}$:

$$\tilde{n}_{\mathrm{SP}} = \Phi(z). \quad (2.24)$$

Therefore, shifting this field, $\tilde{n} \to \tilde{n} + \Phi$, so that

$$\langle\tilde{n}\rangle_z := \mathrm{Tr}[\tilde{n}\exp(-\mathcal{J}_z)] = 0 \quad (2.25)$$

the harmonic (Gaussian) part of $\mathcal{J}_z$ becomes

$$\begin{aligned}\mathcal{J}_z^{(0)} &= \int d^dx\Big\{\lambda\int dt\tilde{n}[\lambda^{-1}\partial_t - \nabla^2 + (r-g\Phi)]n \\ &\quad + \frac{c\Phi}{2}(\nabla m_\infty)^2 + \frac{\Phi}{2}(g'+f\Phi)m_\infty^2 \\ &\quad + \left(z + r\Phi - \frac{g}{2}\Phi^2\right)m_\infty\Big\}. \quad (2.26)\end{aligned}$$

Here we have implied that the saddle-point value of m_∞ is zero; i.e., we have to assume that $\rho = (g'+f\Phi)\Phi$ is positive. If $\rho = 0$, which is the case near the tricritical instability of our stochastic process, a phase transition to a positive value of $\langle m_\infty\rangle$ sets in. Whether or not this transition is the anticipated collapse transition deserves further scrutiny. A shift

$$\tilde{n} \to \tilde{n} + \alpha m_\infty \quad (2.27)$$

[which does not change the condition (2.25)] changes $\Phi(g'+f\Phi)$ to $\Phi(g'+f\Phi)+\alpha\tau$, where $\tau = r - g\Phi$. The special value $\alpha = -c\Phi/2$ eliminates the gradient term $\sim(\nabla m_\infty)^2$, and hence $\rho = 0$ signals the collapse only if τ goes to zero, which is indeed the critical value corresponding to large clusters

with $N \gg 1$. This can be seen from the saddle-point condition $h = z + r\Phi - g\Phi^2/2 = 0$, which leads to

$$g\Phi(z) = r - \sqrt{r^2 + 2gz}. \tag{2.28}$$

Thus, the mean-field solution shows a branch-point singularity at $z_c = -r^2/2g$, and $\tau(z) = \sqrt{r^2 + 2gz}$ becomes zero at this singularity.

Until now we have kept the gradient term proportional to c in our theory. The discussion in the last paragraph revealed that this term is redundant in the sense of field theory as it can be eliminated via the shift transformation (2.27). Hence, we will formally set $c = 0$ unless noted otherwise.

Next, let us calculate $\mathcal{P}(N)$ from Eq. (2.23). Inserting $\Phi(z)$ from Eq. (2.28), we easily obtain the probability density of branched polymers with size N in mean-field approximation,

$$\mathcal{P}(N) = \frac{q}{\sqrt{2\pi g}} N^{-3/2} \exp\left(\frac{rq}{g} - \frac{r^2}{2g}N - \frac{q^2}{2g}N^{-1}\right). \tag{2.29}$$

The maximum of this distribution is found at $N = N_0 = q/r$. For $N \gg q/r$, the distribution drops down exponentially. However, this is the region of rare events of our stochastic process where the large branched polymers are found. Hence, small q means effectively $q \ll rN$, and $q = 1$ is "small" in this region. Combining Eqs. (2.2) and (2.18), we obtain the asymptotic result

$$\mathcal{P}(N) \sim N^{-3/2} \exp(-r^2 N/2g), \tag{2.30}$$

and the well-known mean-field animal exponent $\theta = 5/2$ common to the swollen phase, the percolation point, as well as the collapse transition line.

Now, we calculate the monomer distribution (the distribution of the debris particles) of a single large cluster rooted at the point $\mathbf{r} = 0$. We recall from our remarks above that such a root is represented field theoretically by an insertion of the field $\tilde{n}(0,0)$. According to Eq. (2.15), the monomer distribution is given by the inverse Laplace transformation of the correlation function calculated with the harmonic response functional (2.26):

$$\begin{aligned}\langle m_\infty(\mathbf{r})\tilde{n}(0,0)\rangle_z = G_{1,1}(\mathbf{r};z) &= \int_{\mathbf{k}} \frac{\exp(i\mathbf{k}\cdot\mathbf{r})}{\tau(z) + \mathbf{k}^2} \\ &= \int_0^\infty \frac{ds}{(4\pi s)^{d/2}} \exp[-s\tau(z) - \mathbf{r}^2/4s].\end{aligned} \tag{2.31}$$

It follows that

$$\begin{aligned}G_N(\mathbf{r}) &= \frac{1}{\mathcal{P}(N)} \int_{\sigma-i\infty}^{\sigma+i\infty} \frac{dz}{2\pi i}\, e^{zN} G_{1,1}(\mathbf{r};z) \\ &= \frac{g}{(4\pi)^{d/2}} \int_0^\infty \frac{ds}{s^{d/2-1}} \exp(-gs^2/2N - \mathbf{r}^2/4s).\end{aligned} \tag{2.32}$$

This function can be written in terms of generalized hypergeometric series ${}_0F_2$; however, we prefer the integral representation shown in Eq. (2.32). Easily we verify the sum rule

$$\int d^d r\, G_N(\mathbf{r}) = N. \tag{2.33}$$

The radius of gyration R_N can be calculated straightforwardly from its definition,

$$R_N^2 = \frac{1}{Nd} \int d^d r\, G_N(\mathbf{r})\mathbf{r}^2 = \left(2\pi N/g\right)^{1/2}. \tag{2.34}$$

Hence, the gyration exponent is $\nu_A = 1/4$ as anticipated. The integral representation (2.32) yields the asymptotic forms of the monomer distribution for $|\mathbf{r}| \ll R_N$

$$G_N(\mathbf{r}) \sim \frac{1}{|\mathbf{r}|^{d-4}} \tag{2.35}$$

and

$$G_N(\mathbf{r}) \sim \frac{N}{R_N^d} \left(\frac{R_N}{|\mathbf{r}|}\right)^{(d-2)/3} \exp\left[-\frac{3\pi^{1/3}}{4}\left(\frac{|\mathbf{r}|}{R_N}\right)^{4/3}\right] \tag{2.36}$$

if $|\mathbf{r}| \gg R_N$. We see that the monomer distribution in the fractal interior of the cluster has a fractal dimension $d_f = 4$ independent of N. The distribution in the outer region drops down exponentially in $|\mathbf{r}|$, however, with an exponent $4/3 = 1/(1-\nu_A)$. Besides the exponential factor, the distribution decreases algebraically with an exponent $(d-2)/3 = (d/2 - d\nu_A + 2 - \theta)/(1-\nu_A)$. We will show later that these scaling relations comprising the independent critical exponents θ and ν_A hold generally and are not restricted to the mean-field approximation.

Another interesting quantity is the correlation of two roots. Evidently either two roots can belong to one cluster or they can belong to two separate clusters. Their correlation function is of some value in polymer physics because it determines the second virial coefficient of the equation of state of a dilute solution of branched polymers. The connected part of this correlation function, i.e., the cumulant, is given by

$$\begin{aligned}\langle \tilde{n}(\mathbf{r},0)\tilde{n}(0,0)\rangle_z^{(\mathrm{cum})} = C(\mathbf{r};z) &= -\rho \int_{\mathbf{k}} \frac{\exp(i\mathbf{k}\cdot\mathbf{r})}{[\tau(z) + \mathbf{k}^2]^2} \\ &= -\rho \int_0^\infty \frac{ds}{(4\pi s)^{d/2}} s \exp[-s\tau(z) - \mathbf{r}^2/4s].\end{aligned} \tag{2.37}$$

Inverse Laplace transformation leads to

$$\begin{aligned}C_N(\mathbf{r}) \sim \frac{-\rho N^{3/2}}{R_N^d} &\left(\frac{R_N}{|\mathbf{r}|}\right)^{(d-4)/3} \\ &\times \exp\left[-\frac{3\pi^{1/3}}{4}\left(\frac{|\mathbf{r}|}{R_N}\right)^{4/3}\right]\end{aligned} \tag{2.38}$$

in the region $|\mathbf{r}| \gg R_N$, where N should be understood here as the total number of monomers. Since the correlation of roots on the same cluster goes down proportionally to the density of monomers on one single cluster, the increasing behavior of the fraction

$$C_N(\mathbf{r})/G_N(\mathbf{r}) \sim -\rho N^{1/2} \left(\frac{|\mathbf{r}|}{R_N}\right)^{2/3} \tag{2.39}$$

results mainly from the interaction of two separate clusters. They are repelling one another if ρ is positive, and attracting one another for negative ρ. The sharp difference between repelling and attracting is a clear signature of the collapse transition located at $\rho = 0$. Note that a contribution to ρ proportional to τ as discussed above leads only to a change

of the pivotal factor $\rho N^{1/2}$ of order 1 since $\tau(z)$ converts to a term $\sim N^{-1/2}$ through the inverse Laplace transformation.

E. Dynamical response functional revisited

Now, we return to our response functional to refine it into a form that suits us best for our actual field theoretic analysis. As discussed above, the gradient term proportional to c is redundant. To eliminate this term, we apply to the field $\tilde{n}$ the shift and mixing transformation

$$\tilde{n}(\mathbf{r},t) \to \tilde{n}(\mathbf{r},t) + \Phi - c\Phi m_\infty(\mathbf{r}), \tag{2.40}$$

where Φ is a free parameter at this stage. Defining in consistency with our mean-field considerations above, $\tau = r - g\Phi$, $\rho = (g' + f\Phi)\Phi - c\Phi\tau$, $h = z + r\Phi - g\Phi^2/2$, the stochastic functional $\mathcal{J}_z$ (2.21) takes the form

$$\mathcal{J}_z = \int d^dx \Big[\lambda \int dt\, \tilde{n}\big(\lambda^{-1}\partial_t + \tau - \nabla^2 + g_2' m - \frac{g_2}{2}\tilde{n} + g_1 m_\infty\big) n + \Big(\frac{\rho}{2} m_\infty^2 + \frac{g_0}{6} m_\infty^3 + h m_\infty\Big)\Big]. \tag{2.41}$$

Here we could have set τ equal to zero by exploiting that Φ is a free parameter. Instead of doing so, we keep τ in our theory as a small free parameter. We will see later that keeping τ comes in handy for renormalization purposes. In Eq. (2.41) we have eliminated couplings that are of more than third order in the fields because they are irrelevant. We do not write in detail the relatively uninteresting relations between the new third-order coupling constants and the old ones. Note that $\mathcal{J}_z$ contains two similar couplings: $g_2'\tilde{n}nm$ and $g_1\tilde{n}nm_\infty$. Whereas the first coupling respects causal ordering, which means that $\tilde{n}$ is separated by an infinitesimal positive time element from the nm part resulting from the Itô calculus [35], the second one respects causality only between $\tilde{n}$ and n. In contrast to the m part, the m_∞ part contains all the n with times that lie in the past and in the future of $\tilde{n}$. This property is the heritage of the time-delocalized noise term. Even if we had disregarded the noise term proportional to f in Eq. (2.12) initially, the $\tilde{n}nm_\infty$ coupling would be generated by coarse graining, and hence it must be ultimatively incorporated into the theory to yield a renormalizable theory.

The relevance of the different terms in $\mathcal{J}_z$ follows from their dimensions with respect to an inverse length scale μ such that time scales as μ^{-2}. Fundamentally, one has to decide which parameters are the critical control parameters going to zero in mean-field theory. As we have seen, at the collapse transition these are $\tau \sim \rho \sim \mu^2$ and $h \sim \mu^{(d+2)/2}$. The dimensions of the fields are then given by $\tilde{n} \sim m \sim \mu^{(d-2)/2}$ and $n \sim \mu^{(d+2)/2}$. It follows that all the coupling constant g_0, g_1, g_2, and g_2' have the same dimension $\mu^{(6-d)/2}$. Note that $\tilde{n}$ is tied always to at least one factor of n as a result of absorptivity of the process. Hence, we have retained all the couplings that are relevant for $d \leqslant 6$ spatial dimensions, and the model is renormalizable below the upper critical dimension $d_c = 6$ of the collapse transition. The situation is different if ρ is a finite positive quantity, that is, in the swollen phase. Then ρ can be absorbed into the fields by a scale transformation that amounts to formally setting $\rho = 2$. The field dimensions then become $m \sim \mu^{d/2}$, $n \sim \mu^{(d+4)/2}$, and $\tilde{n} \sim \mu^{(d-4)/2}$. It follows that $h \sim \mu^{d/2}$, $g_0 \sim \mu^{-d/2}$, $g_1 \sim \mu^{(4-d)/2}$, $g_2' \sim \mu^{(2-d)/2}$, and $g_2 \sim \mu^{(8-d)/2}$. Hence, in the swollen phase only $g_2 = g$ is relevant, now below eight spatial dimensions. The other couplings can be safely removed.

F. Quasistatic limit and ghosts

In the following, we focus on the static properties of the generated clusters after the epidemic has become extinct. Here we are interested only in time-independent static expectation values of the form $\langle \prod_i m_\infty(\mathbf{r}_i) \prod_j \tilde{n}(\mathbf{r}_j,0)\rangle$. Thus, we take the quasistatic limit [18,23,28,31] (see Appendix A) by setting $\tilde{n}(\mathbf{r},t) \to \tilde{n}_0(\mathbf{r}) =: \varphi(\mathbf{r})$ in the dynamic response functional $\mathcal{J}_z$. We rename $m_\infty(\mathbf{r}) =: \tilde{\varphi}(\mathbf{r})$ and get

$$\mathcal{J}_z \to \mathcal{H}_{qs} = \int d^dx \Big[\tilde{\varphi}(\tau - \nabla^2)\varphi + \frac{\rho}{2}\tilde{\varphi}^2 + h\tilde{\varphi} + \frac{g_0}{6}\tilde{\varphi}^3 + g_1\tilde{\varphi}\varphi\cdot\tilde{\varphi} + \frac{1}{2}\tilde{\varphi}(g_2'\tilde{\varphi} - g_2\varphi)\varphi\Big], \tag{2.42}$$

where we have denoted the original time delocalization of the $\tilde{n}nm_\infty$ term by a separating dot in $\tilde{\varphi}\varphi\cdot\tilde{\varphi}$. Using the quasistatic limit, one has to be careful to account for the former causal ordering of fields in the diagrammatic perturbation expansion. This means that one has to rule out diagrams with closed propagator loops. But note that only the $\tilde{\varphi}\varphi$ part of the $\tilde{\varphi}\varphi\cdot\tilde{\varphi}$ term can contribute to such a closed loop.

Of course, these additional rules make the perturbation expansion very clumsy in higher loop-order calculations. Fortunately there exists an elegant way to overcome these difficulties associated with the additional rules by introducing so-called ghost fields, whose sole purpose is to generate additional diagrams that cancel any diagrams with noncausal propagator-loops. Such a procedure does not change the physical content of the theory but simplifies calculations and makes it easier to find higher symmetries. To one-loop order, noncausal loops are easily canceled by a corresponding loop of contrary sign. The ghost fields for producing such loops that come to mind first are a pair of fermionic fields. Note, however, that D independent similar bosons can also create a loop with a negative sign in the limit $D \to -2$ (see Fig. 2).

To be more specific, the ghost fields that we use are D independent bosonic fields $(\psi_1, \ldots, \psi_D)$, in the limit $D \to -2$, which is taken at the end of the calculation. These ghosts are incorporated into our theory by adding the term

$$\frac{1}{2}\sum_{k=1}^{D} \psi_k\{\tau_0 - \nabla^2 + [(g_1 + g_2')\varphi - g_2\tilde{\varphi}]\}\psi_k \tag{2.43}$$

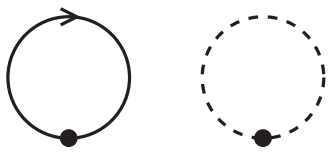

FIG. 2. One-loop noncausal diagrams and their cancellation by $D = -2$ bosonic ghost fields.

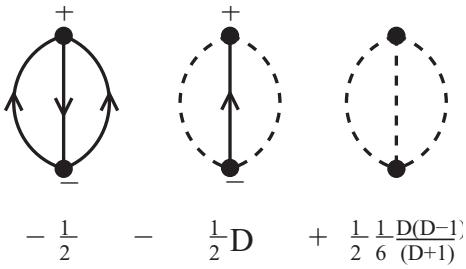

FIG. 3. Basic diagrams for the cancellation of coupled noncausal loops by $D = -2$ bosonic ghosts.

to the integrand of $\mathcal{J}_z$ (2.42). Note that this term arises formally if one replaces each causal ordered $\tilde{n}n$ pair in $\mathcal{J}_z$ by the sum over $\psi_k\psi_k/2$ pairs. Here a new symmetry comes into play: The additional term (2.43) is trivially invariant under any permutation of the D ghost fields ψ_k; i.e., we have symmetry under the permutation (or symmetric) group S_D. However, since in general $\sum_{k=1}^{D}\psi_k \neq 0$, this representation is reducible. Hence, it is more useful to introduce new ghost fields $(\chi_1,\ldots,\chi_{D+1})$ with constraint $\sum_{\alpha=1}^{D+1}\chi_\alpha = 0$, and $\sum_{k=1}^{D}\psi_k^2 = \sum_{\alpha=1}^{D+1}\chi_\alpha^2 =: \chi^2$. This is easily achieved by using $D+1$ Potts spin vectors $\vec{e}^{(\alpha)} = (e_k^{(\alpha)})$ directed to the corners of a D-dimensional simplex. The spin vectors have the usual properties: $\sum_{\alpha=1}^{D+1} e_k^{(\alpha)} = 0$, $\sum_{\alpha=1}^{D+1} e_i^{(\alpha)} e_k^{(\alpha)} = \delta_{ik}$, $\sum_{k=1}^{D} e_k^{(\alpha)} e_k^{(\beta)} = \delta_{\alpha\beta} - 1/(D+1)$. Hence, the relation between the old and the new ghosts is given by $\chi_\alpha = \sum_{k=1}^{D} e_k^{(\alpha)}\psi_k$. Now, we have symmetry under the permutation group S_{D+1} of permutations of the $(D+1)$ ghost fields χ_α, and this representation is irreducible.

Inspection shows that the ghosts also work in multiloop diagrams provided that the noncausal loops are separated from each other in these diagrams [18]. However, as long as g_2' is not zero (note that g_2 is always greater than zero because otherwise only diagrams without loops are generated), nonseparated noncausal loops arise; see the first diagram in Fig. 3. The cancellation requires a permutation-symmetric irreducible interaction $\chi^3 = \sum_{\alpha=1}^{D+1}\chi_\alpha^3$ of the $(D+1)$ ghosts; see the third diagram in Fig. 3. Using these new ghosts, the quasistatic Hamiltonian becomes

$$\mathcal{H} = \int d^dx \Big\{ \tilde{\varphi}(\tau - \nabla^2)\varphi + \frac{\rho}{2}\tilde{\varphi}^2 + h\tilde{\varphi} + \frac{1}{2}[\tau\chi^2 + (\nabla\chi)^2] + \frac{g_0}{6}\tilde{\varphi}^3 + \frac{g_1}{2}\tilde{\varphi}(2\tilde{\varphi}\varphi + \chi^2) + \frac{1}{6}[3\tilde{\varphi}(g_2'\tilde{\varphi} - g_2\varphi)\varphi + 3(g_2'\tilde{\varphi} - g_2\varphi)\chi^2 + \sqrt{g_2' g_2}\,\chi^3] \Big\}. \quad (2.44)$$

Perturbation theory with this Hamiltonian is no longer burdened with additional rules. It will serve as the vantage point of our RG calculations. As it stands, it is general enough to capture both the swollen phase and the collapse transition. As we have shown in mean-field theory, the collapse transition corresponds to vanishing τ, ρ, and h. Swollen RBPs correspond to vanishing τ and h, but positive and finite ρ.

The Hamiltonian (2.44) is form invariant under three transformations of the fields. Therefore, three parameters of the Hamiltonian are redundant. One of these transformations, the mixing $\varphi \to \varphi + \kappa\tilde{\varphi}$, $\tilde{\varphi} \to \tilde{\varphi}$, we have already used to eliminate the gradient term $(\nabla\tilde{\varphi})^2$. The second of these transformations, the rescaling $\varphi \to \lambda\varphi$, $\tilde{\varphi} \to \lambda^{-1}\tilde{\varphi}$, can be used either to identify coupling-constants $g_2' = g_2$ or to transform g_2 to one and use only scaling-invariant quantities. Via the third transformation, the shift $\varphi \to \varphi + \gamma$, $\tilde{\varphi} \to \tilde{\varphi}$, either τ or ρ can be transformed away. At this point a word of caution is in order. Using these transformations to eliminate parameters from the field theoretic functional, one is well advised to make sure that none of the parameters κ, λ, or γ featured in the transformations is singular. Otherwise, parameters eliminated from the unrenormalized theory will have to reemerge in the renormalization procedure. This is no problem per se, but it is a fact that can be easily overlooked and, if so, will lead to ill-defined renormalization schemes.

Before moving on to our actual RG calculation, we find it worthwhile to comment on the renormalizability of $\mathcal{H}$. Simple power counting shows that the ghosts have the same dimensionality as the fields $\tilde{\varphi}$ and φ, namely, $\chi_\alpha \sim \mu^{(d-2)/2}$. For the swollen phase, the coupling constants g_0, g_1, and g_2' are irrelevant and hence can and should be set equal to zero. Then one can easily ascertain that the remaining $\mathcal{H}$ contains all the relevant terms generated under renormalization, and hence $\mathcal{H}$ is renormalizable as far as the swollen phase is concerned. For the collapse transition, the situation is more intricate. Simple inspection by means of power counting lends credence to the renormalizability of $\mathcal{H}$. However, one has to be more careful here because of the way the various g appear in multiple places; i.e., a given g may appear as a factor of different monomials of the fields, namely, in couplings among the ghost, in couplings among the primary fields φ and $\tilde{\varphi}$, and in couplings of the primary fields and the ghosts. Does this spoil renormalizability? The answer is clearly *no* because we know for certain that $\mathcal{H}$ is renormalizable by virtue of its equivalence in the quasistatic limit to the renormalizable dynamic functional $\mathcal{J}_z$, which is renormalizable. Hence, there must exist some hidden symmetry that masks the renormalizability of $\mathcal{H}$. Once revealed, this underlying symmetry will provide for relations between different vertex functions. We will show shortly that this is the symmetric group S_{D+2} (not only the permutation symmetry S_{D+1} of the $D+1$ ghosts alone) of the permutation of $(D+2)$ field combinations. First, however, we will look briefly at a one-loop calculation that underpins and exemplifies the considerations just presented.

G. One-loop diagrams with ghosts

The elements of our diagrammatic perturbation expansion, the propagators, the correlators, and the vertices, are listed in Figs. 4 and 5, respectively. For now, we focus just on the decorations of Feynman diagrams, i.e., the combinations of coupling constants and symmetry factors of the diagrams without the integrations over loop momenta. We list the

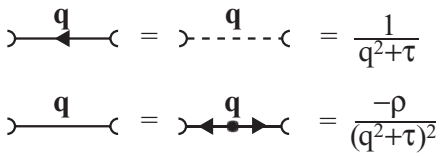

FIG. 4. Propagators and correlators.

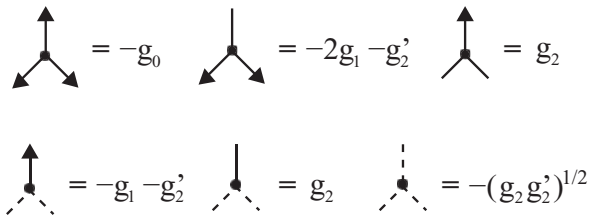

FIG. 5. Vertices.

relevant one-loop diagrams, writing them in a form that makes evident the cancellations in the limit $D \to -2$. For the tadpole diagrams (Fig. 6), we find

$$(1a): \quad g_2 + \frac{D}{2} g_2 \to 0, \tag{2.45a}$$

$$(1b): \quad -\left[g_1 + (g_1 + g_2')\right] - \frac{D}{2}(g_1 + g_2') \to -g_1. \tag{2.45b}$$

The self-energy diagrams (Fig. 7) yield

$$(2a): \quad g_2^2 + \frac{D}{2} g_2^2 \to 0, \tag{2.46a}$$

$$(2b): \quad -\frac{1}{2} g_2(2g_1 + g_2') - g_2[g_1 + (g_1 + g_2')] - \frac{D}{2} g_2(g_1 + g_2') \to -2g_1 g_2 - \frac{1}{2} g_2 g_2', \tag{2.46b}$$

$$(2c): \quad -g_0 g_2 + [g_1 + (g_1 + g_2')]^2 + \frac{D}{2}(g_1 + g_2')^2 \to -g_0 g_2 + 3g_1^2 + 2g_1 g_2'. \tag{2.46c}$$

In the same way we obtain the decorations of the vertex diagrams (Figs. 8–11):

$$(3a): \quad 2g_2^3 + D g_2^3 \to 0, \tag{2.47a}$$

$$(3b): \quad -2g_2^2(2g_1 + g_2') - 2g_2^2[g_1 + (g_1 + g_2')] - D g_2^2(g_1 + g_2') \to -6g_1 g_2^2 - 2g_2^2 g_2', \tag{2.47b}$$

$$(3c): \quad 2g_2(2g_1 + g_2')^2 - 2g_0 g_2^2 + 2g_2[g_1 + (g_1 + g_2')]^2 + D g_2(g_1 + g_2')^2 \to 14 g_1^2 g_2 + 12 g_1 g_2 g_2' + 2 g_2 g_2'^2 - 2 g_0 g_2^2, \tag{2.47c}$$

$$3d): \quad 6g_0 g_2(2g_1 + g_2') - 2[g_1 + (g_1 + g_2')]^3 + 2D(g_1 + g_2')^3 \to 12 g_0 g_1 g_2 + 6 g_0 g_2 g_2' - 14 g_1^3 - 18 g_1^2 g_2 g_2' - 6 g_1 g_2'^2. \tag{2.47d}$$

Of course, the cancellation of noncausal loops (see Fig. 2) should occur also in higher loop orders. Hence, not only the propagator and the ghost correlator must be equal but also the full Green's functions $\langle \varphi(\mathbf{r})\tilde{\varphi}(\mathbf{0})\rangle$ and $\langle \chi(\mathbf{r})\chi(\mathbf{0})\rangle$. Therefore, the one-loop self-energy diagrams ($2b$) shown in Fig. 7 must

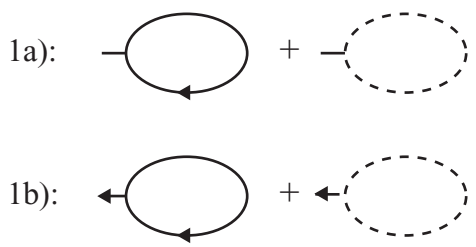

FIG. 6. One-loop tadpole diagrams.

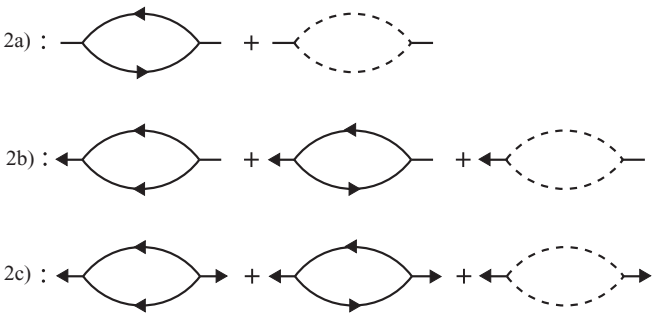

FIG. 7. One-loop self-energy diagrams.

be equal to the one-loop self-energy diagrams ($2d$) of the ghost shown in Fig. 12:

$$2d) \;= -2g_2(g_1 + g_2') + \frac{1}{2}\left(\frac{D-1}{D+1}\right) g_2 g_2' \to -2g_1 g_2 - \frac{1}{2} g_2 g_2' = 2b). \tag{2.48}$$

Hence, the $\sim\chi^3$ self-interaction of ghosts featured in $\mathcal{H}$ is needed already at one-loop order to guarantee the equality of self-energies.

H. Hidden symmetry and relation to other models

Now, we come back to the search for the symmetry that ensures the renormalizability of the Hamiltonian $\mathcal{H}$ [Eq. (2.44)]. At first glance, this Hamiltonian has only the permutation symmetry S_{D+1} of the $(D+1)$ ghost fields (χ_α). Next we use the form invariance of the Hamiltonian under a rescaling of the original fields

$$\varphi \to \lambda\varphi, \qquad \tilde{\varphi} \to \lambda^{-1}\tilde{\varphi}, \tag{2.49}$$

which is compensated for and hence becomes a scaling symmetry when augmented by the following redefinition of parameters:

$$g_0 \to \lambda^3 g_0, \quad g_1 \to \lambda g_1, \quad g_2' \to \lambda g_2', \quad g_2 \to \lambda^{-1} g_2, \quad \rho \to \lambda^2 \rho, \quad h \to \lambda h. \tag{2.50}$$

Under the choice $\lambda = \sqrt{g_2'/g_2}$, which is possible as long as $g_2' \neq 0$, we gain the equality $g_2' = g_2$. Now, it is easy to show that the Hamiltonian $\mathcal{H}$ is invariant for each $\alpha = 1, \ldots, D+1$ under the mirror transformations

$$\tilde{\varphi} \to \tilde{\varphi}, \qquad \varphi \to (\varphi - \tilde{\varphi}) - \chi_\alpha, \qquad \chi_\alpha \to -\chi_\alpha - 2\tilde{\varphi}, \quad \chi_\beta \to (\chi_\beta - \chi_\alpha) - \tilde{\varphi}, \tag{2.51}$$

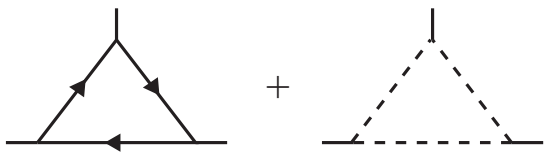

FIG. 8. One-loop vertex diagrams (a).

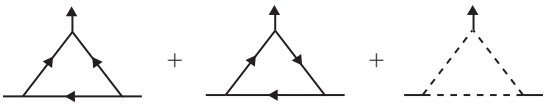

FIG. 9. One-loop vertex diagrams (b).

for all $\beta \neq \alpha$, and always in the limit $D \to -2$. This invariance ensures, e.g., the equality of the ghost correlation functions with the propagator

$$\langle \chi_\alpha \chi_\beta \rangle = \left(\delta_{\alpha\beta} - \frac{1}{D+1} \right) \langle \varphi \tilde{\varphi} \rangle \tag{2.52}$$

that we have demonstrated explicitly to one-loop order above. The mirror transformations that mix original fields with ghosts complete the permutation symmetries of the ghosts to the full symmetry group S_{D+2}.

To make this hidden symmetry more transparent, we define a new order parameter field with $(D+3)$ components: $s_0 = \tilde{\varphi}$, $s_1 = -\varphi$, and for $\mu \geqslant 2$: $s_\mu = \chi_{\mu-1} - (\tilde{\varphi} - \varphi)/(D+1)$. With $s^k := \sum_{\mu=0}^{n} s_\mu^k$, where $n = D+2$, we have $s^1 = 0$, and in the limit $n \to 0$:

$$s^2 = 2\tilde{\varphi}\varphi + \chi^2, \tag{2.53a}$$

$$s^3 = 3\tilde{\varphi}(\tilde{\varphi} - \varphi)\varphi + 3(\tilde{\varphi} - \varphi) + \chi^3. \tag{2.53b}$$

Using this order parameter, it is easy to see that the Hamiltonian can be written as

$$\mathcal{H}_{\mathrm{aP}} = \int d^d x \left\{ \frac{1}{2}[\tau s^2 + (\nabla s)^2] + \frac{\rho}{2} s_0^2 + h s_0 + \frac{g_0}{6} s_0^3 + \frac{g_1}{2} s_0 s^2 + \frac{g_2}{6} s^3 \right\}, \tag{2.54}$$

which is identical to the Hamiltonian of Eq. (2.44) in the limit $n \to 0$. It is therefore equivalent to our original dynamical model. The Hamiltonian $\mathcal{H}_{\mathrm{aP}}$ describes the field theory of the asymmetric $(n+1)$-state Potts model. The previously hidden symmetry is now the symmetry S_n of permutations of the n fields $(s_1, \ldots s_n)$. As mentioned in Sec. I, the established theories for RBPs [1,3,15] are mainly based on the asymmetric Potts model, and the Hamiltonian (2.54) therefore establishes the connection with these theories. Note, furthermore, that for $g_0 = g_1 = 0$ the Hamiltonian (2.54) describes the symmetric $(n+1)$-state Potts model with a linear and quadratic (so-called hard) symmetry breaking. The interaction represented by the third-order terms has S_{n+1} symmetry and yields the field theory of percolation in the limit $n \to 0$. There exists

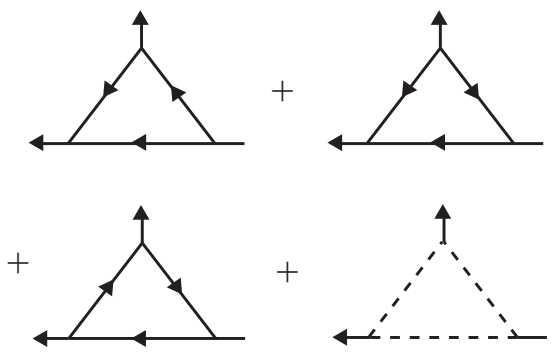

FIG. 10. One-loop vertex diagrams (c).

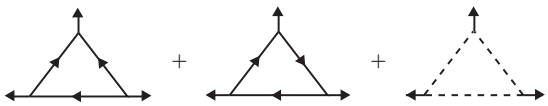

FIG. 11. One-loop vertex diagrams (d).

another connection: One can show that for $4g_0 = 2g_1 = -g_2$ the Hamiltonian $\mathcal{H}_{\mathrm{aP}}$ decomposes in a sum of n uncoupled Hamiltonians, each describing the Yang-Lee edge problem. The choice of these special combinations of coupling constants yields important checks for higher-order calculations [37].

Now, we turn to the case that g_2' is zero, where we cannot rescale the fields to attain $g_2' = g_2$. As we will show, g_2' becomes zero at the fixed point of our model for the collapse, and it is irrelevant for the model in the swollen phase of the RBP. Hence, the case $g_2' = 0$ is important in general for the statistics of branched polymers. Now the third-order coupling $\sim \chi^3$ of the ghosts in $\mathcal{H}$ [Eq. (2.44)] vanishes. The ghosts appear only quadratic, and we can integrate them out formally producing a ghost determinant raised to the power $(-D/2)$. Taking the limit $D \to -2$, this determinant can be reimported into the Hamiltonian by introducing a pair $(\bar{\psi}, \psi)$ of anticommuting fermionic ghost fields. The Hamiltonian becomes

$$\mathcal{H}_{\mathrm{ss}} = \int d^d x \left[\tilde{\varphi}(\tau - \nabla^2)\varphi + \frac{\rho}{2}\tilde{\varphi}^2 + h\tilde{\varphi} + \bar{\psi}(\tau - \nabla^2 + g_1\tilde{\varphi} - g_2\varphi)\psi + \frac{g_0}{6}\tilde{\varphi}^3 + g_1\tilde{\varphi}^2\varphi - \frac{g_2}{2}\tilde{\varphi}\varphi^2 \right]. \tag{2.55}$$

Introducing Grassmannian anticommuting supercoordinates θ, $\bar{\theta}$ with integration rules $\int d\theta\, 1 = \int d\bar{\theta}\, 1 = 0$, $\int d\theta\, \theta = \int d\bar{\theta}\, \bar{\theta} = 1$, and defining a superfield $\Phi(\mathbf{r}, \bar{\theta}, \theta) = i\varphi(\mathbf{r}) + \bar{\theta}\psi(\mathbf{r}) + \bar{\psi}(\mathbf{r})\theta + i\bar{\theta}\theta\tilde{\varphi}(\mathbf{r})$, the Hamiltonian $\mathcal{H}_{\mathrm{ss}}$ takes the form

$$\mathcal{H}_{\mathrm{ss}} = \int d^d x d\bar{\theta} d\theta \left\{ \frac{1}{2}\Phi(\tau - \nabla^2 - \rho\partial_{\bar{\theta}}\partial_\theta)\Phi + ih\Phi + i\left[\frac{g_2}{6}\Phi^3 + \frac{g_1}{2}\Phi^2(\partial_{\bar{\theta}}\partial_\theta\Phi) - \frac{g_0}{6}\Phi(\partial_{\bar{\theta}}\partial_\theta\Phi)^2 \right] \right\}. \tag{2.56}$$

This Hamiltonian shows (BRS) symmetry [25,27]; i.e., $\mathcal{H}_{\mathrm{ss}}$ is invariant under a supertranslation $\theta \to \theta + \varepsilon$, $\bar{\theta} \to \bar{\theta} + \bar{\varepsilon}$. Moreover, if the control parameter ρ is positive and finite, i.e., if we consider the problem of swollen RBPs, ρ can be reset by a scale transformation of the supercoordinates to two. The supercoordinates get a dimension $\sim \mu^{-1}$ equal to the dimension of the spatial coordinates, and the derivatives combine to a super-Laplace operator $\nabla^2 + \rho\partial_{\bar{\theta}}\partial_\theta \to \nabla^2 + 2\partial_{\bar{\theta}}\partial_\theta =: \Box$. As we have shown above, the coupling constants

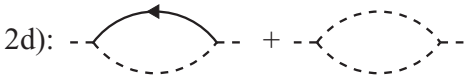

FIG. 12. One-loop self-energy diagrams of ghosts.

g_0 and g_1 become irrelevant and hence can be neglected, in which case the Hamiltonian takes the super-Yang-Lee form

$$\mathcal{H}_{\mathrm{sYL}} = \int d^d x d\bar{\theta} d\theta \left[\frac{1}{2}\Phi(\tau - \Box)\Phi + i\frac{g}{6}\Phi^3 + ih\Phi \right], \tag{2.57}$$

where we have set $g_2 = g$. The Hamiltonian $\mathcal{H}_{\mathrm{sYL}}$ has, besides the supertranslation invariance, superrotation invariance. Now dimensional reduction can be used to reduce the problem to the normal Yang-Lee problem in two lesser dimensions. This establishes the connection between our model and the work of Parisi and Sourlas [4] on swollen RBPs.

Before moving on to the core of our RG analysis, we would like to highlight the following implication of our symmetry considerations for the collapse transition. We will see later that g_2' vanishes at the RG fixed point describing the θ transition. Thus, this transition is associated with BRS symmetry, which is in contrast to the swollen phase, which is associated with full supersymmetry. The BRS symmetry indicates that the statistics of the RBPs is dominated by tree configurations.This fact can be understood, for example, by using Cardy's presentation [21] of the work of Brydges and Imbrie [20]. Cardy reformulates their model of swollen RBPs in d dimensions (which is exactly reducible to the problem of the universal repulsive gas singularity in $d-2$ dimensions, which, in turn, belongs to the same universality class as the Yang-Lee problem) in a fully supersymmetric way. If one adds an attracting potential between the monomers of the tree polymers that can lead eventually to the collapse of the RBPs, the rotational supersymmetry is lost, and with it dimensional reduction. However, BRS symmetry is retained, and this symmetry is indeed the vehicle that reduces all configurations to trees. Another route to understand the connection between BRS symmetry and trees lies in a dynamical calculation. At first, this may sound somewhat surprising because BRS symmetry is a feature of the quasistatic Hamiltonian at the collapse fixed point. However, a calculation [37] of the fractal dimension of the minimal path from the original dynamic model (2.41) with $g_2' = 0$ clearly shows that the backbone of the RBPs is topologically one-dimensional. Thus, asymptotically large RBPs at the θ transition have the topology of trees.

III. RENORMALIZATION AND THE RENORMALIZATION GROUP

Now, we turn to the core of our RG analysis. As announced above, we will base our discussion on the Hamiltonian $\mathcal{H}$ of Eq. (2.44). Likewise, we could use $\mathcal{H}_{\mathrm{aP}}$ with the limit $n \to 0$, which, as we have shown above, is equivalent to $\mathcal{H}$. For our discussion here, we choose $\mathcal{H}$ over $\mathcal{H}_{\mathrm{aP}}$ because we believe that the relation of the former to the original GEP is somewhat more intuitive than that of the latter. Actual diagrammatic calculations in higher loop orders, however, are better to handle when $\mathcal{H}_{\mathrm{aP}}$ instead of $\mathcal{H}$ is used. The renormalization-group functions that feed into our RG analysis for RBPs stem from a renormalized field theoretic calculation for the asymmetric Potts model that we performed recently. Details of this work will be presented elsewhere [37].

A. The renormalization scheme

Our main focus here lies on the collapse transition; i.e., we are mainly interested in the case that the control parameters τ and ρ take critical values (zero in mean-field theory) where the correlation length diverges, and correlations between different polymers vanish. Via the equation of state this implies the critical value of h. The principal objects of the perturbation theory are the superficially UV-divergent vertex functions $\Gamma_{\tilde{k},k}$, which consist of irreducible diagrams with $\tilde{k}$ and k amputated legs of $\tilde{\varphi}$ and φ, respectively, as functions of the wavevector $\mathbf{q}$. The UV divergences are then handled via a renormalization scheme that introduces counter terms that absorb said divergences. For our calculations we use minimal renormalization, i.e., dimensional regularization and minimal subtraction in conjunction with the ε expansion about $d = 6$ dimensions ($\varepsilon = 6 - d$). Our renormalization scheme leading from bare to renormalized quantities reads

$$(\tilde{\varphi},\varphi,\chi) \to (\mathring{\tilde{\varphi}},\mathring{\varphi},\mathring{\chi}) = Z^{1/2}(\tilde{\varphi},\varphi + K\tilde{\varphi},\chi), \tag{3.1a}$$

$$\underline{\tau} \to \underline{\mathring{\tau}} = Z^{-1}\underline{\underline{Z}} \cdot \underline{\tau} + \underline{\mathring{\tau}}_c, \tag{3.1b}$$

$$h \to \mathring{h} = Z^{-1/2}\left(h + \tfrac{1}{2}G_\varepsilon^{1/2}\mu^{-\varepsilon/2}\underline{\tau} \cdot \underline{\underline{A}} \cdot \underline{\tau}\right) + \underline{\mathring{C}}_c \cdot \underline{\tau} + \mathring{h}_c, \tag{3.1c}$$

$$G_\varepsilon^{1/2} g_\alpha \to G_\varepsilon^{1/2}\mathring{g}_\alpha = Z^{-3/2}(u_\alpha + B_\alpha)\mu^{\varepsilon/2}, \tag{3.1d}$$

where G_ε is a convenient numerical factor that we choose here to be $G_\varepsilon = \Gamma(1+\varepsilon/2)/(4\pi)^{d/2}$. Note, however, that all choices with $(4\pi)^3 G_\varepsilon = 1 + O(\varepsilon)$ work equally well since their differences amount only to a finite rescaling of the momentum scale μ. We introduce the two-dimensional control vector $\underline{\tau} = (\rho,\tau)$ and $(g_\alpha) = (g_0,g_1,g_2',g_2)$. In a theory regularized by means of a large momentum cutoff Λ, the additive nonuniversal counter terms $\underline{\mathring{\tau}}_c$, $\mathring{h}_c$, and $\underline{\mathring{C}}_c$ would diverge $\sim \Lambda^2$, $\Lambda^{4-\varepsilon/2}$ and $\Lambda^{2-\varepsilon/2}$. In our perturbative approach based on dimensional regularization and minimal subtraction with ε expansion, they formally vanish. In minimal renormalization, all the other counterterms are expanded into pure Laurent series, e.g.,

$$Z - 1 = \frac{Z^{(1)}}{\varepsilon} + O(\varepsilon^{-2}), \tag{3.2a}$$

$$K = \frac{K^{(1)}}{\varepsilon} + O(\varepsilon^{-2}), \tag{3.2b}$$

and so on, where the residua $Z^{(1)}$, $K^{(1)}$, . . . of the ε poles are pure functions of the dimensionless renormalized coupling constants $(u_\alpha) = (u_0,u_1,u_2',u_2)$. We present the calculation of all the counterterms to one-loop order in Appendix B.

Note that the renormalization scheme (3.1) introduces a counterterm proportional to K that has no counterpart in the Hamiltonian (2.44). This counterterm can be viewed as a remnant of the gradient term proportional to the redundant parameter c in the original response functional (2.13), which we removed from our model via the mixing transformation stated in Eq. (2.40). As a counterterm this term is

indispensable, however, because the quadratically superficial divergent vertex function

$$\Gamma_{2,0}(\mathbf{q}) = \Gamma_{2,0}(\mathbf{0}) + \mathbf{q}^2\Gamma''_{2,0}(\mathbf{0}) + \cdots \tag{3.3}$$

contains an UV-divergent $\Gamma''_{2,0}(\mathbf{0})$. This fact was overlooked by LI [1] in their calculation, and their long-standing one-loop results are incorrect, although, fortunately, the numeric deviations from the correct one-loop results are rather small. It must be stressed, however, that the omission of this counterterm is not just a technical glitch that affects some numbers. Without this term, renormalization does not cure the theory from nonprimitive divergences and is thus not really meaningful. In a one-loop calculation one does not see these nonprimitive divergences explicitly, and hence they are easily overlooked. At higher loop order, however, they inevitably pop up, and one can see explicitly and in detail how the theory fails if not renormalized properly.

The alert reader might ask why the different fields are renormalized with the same renormalization factor Z. The fields belong to two different irreducible representations of the symmetry group S_n, mathematically denoted by $\{n\}$ and $\{n-1,1\}$, the trivial and the fundamental representations, respectively. They should therefore require two independent factors Z_0 and Z_1. In general, this argumentation is correct, and $Z_0 \neq Z_1$ as long as $n \neq 0$ as well as g_0 or g_1 are nonzero. In the limit $n \to 0$, however, these renormalization factors become equal. To demonstrate this, we reduce the order parameter $s = [s_0 = \tilde{\varphi}, s_1 = -\varphi, s_{\alpha+1} = \chi_\alpha + (\varphi - \tilde{\varphi})/(n-1)]$ of the Hamiltonian $\mathcal{H}_{\mathrm{aP}}$ (2.54) into its irreducible components:

$$\phi_0 = \sqrt{\frac{n+1}{n}}\, s_0 \in \{n\}, \tag{3.4a}$$

$$\phi_\nu = s_\nu + \frac{1}{n} s_0 \in \{n-1,1\}, \tag{3.4b}$$

with $\sum_{\nu=1}^{n} \phi_\nu = 0$, and $s^2 = \phi_0^2 + \phi^2$. The renormalizations

$$\phi_0 \to \mathring{\phi}_0 = Z_0^{1/2}\phi_0, \tag{3.5a}$$

$$\phi_\nu \to \mathring{\phi}_\nu = Z_1^{1/2}\phi_\nu \tag{3.5b}$$

lead to

$$s_0 \to \mathring{s}_0 = Z_0^{1/2} s_0, \tag{3.6a}$$

$$s_\nu \to \mathring{s}_\nu = Z_1^{1/2} s_\nu + \frac{1}{n}\left(Z_1^{1/2} - Z_0^{1/2}\right) s_0. \tag{3.6b}$$

We know that these last two renormalizations stay finite in the limit $n \to 0$ since our primary Hamiltonian (2.44) is renormalizable. Hence,

$$\lim_{n\to 0} Z_0 = \lim_{n\to 0} Z_1 = Z, \tag{3.7a}$$

$$\lim_{n\to 0}\left[\frac{(Z_0/Z_1)^{1/2} - 1}{n}\right] = K, \tag{3.7b}$$

which leads back to the renormalizations (3.1a). This discussion sheds another light on what went wrong in the calculation by LI. They overlooked that Z_0 and Z_1 approach their limit Z differently, as manifested in Eq. (3.7b). This difference, when overlooked, leads to erroneous results.

The bare Hamiltonian (2.44) is form invariant under a rescaling of the fields that makes one of the coupling constants redundant. This rescaling can be chosen in particular so that $\mathring{g}'_2 = \mathring{g}_2$ [see the discussion after Eqs. (2.49) and (2.50)], which leads to the Hamiltonian (2.54) in the form of the asymmetric Potts model. Owing to the permutation symmetry S_n of this Hamiltonian, this relation holds even in renormalized form, $u'_2 = u_2$, where u_2 is related to the bare $\mathring{g}_2$ by the renormalization factor Z_2. It follows the relation

$$\frac{B'_2}{u'_2} = \frac{B_2}{u_2} =: Z_2 - 1, \tag{3.8}$$

where Z_2 depends only on scaling invariant combinations of the coupling constants, say,

$$u = u_2 u'_2, \tag{3.9a}$$

$$v = u_1 u_2, \tag{3.9b}$$

$$w = u_0 u_2^3. \tag{3.9c}$$

B. Shift symmetry and Ward identities

The Hamiltonian (2.44) is, as typical for a ϕ^3 theory, form invariant under a shift of the order parameter by an arbitrary constant. To be more specific, the Hamiltonian is form invariant under

$$\varphi \to \varphi' = \varphi + \gamma \tag{3.10}$$

in conjunction with the parameter change:

$$\tau \to \tau' = \tau + g_2\gamma, \tag{3.11a}$$

$$\rho \to \rho' = \rho - (2g_1 + g'_2)\gamma, \tag{3.11b}$$

$$h \to h' = h - \tau\gamma - \frac{g_2}{2}\gamma^2. \tag{3.11c}$$

Note that the coupling constants are not transformed. Hence, the primed fields and parameters are renormalized with the same counterterms as the original ones. Thus, the transformations represent a scaling symmetry in renormalized as well as in bare form. We introduce the two-dimensional vector $\underline{f} = (-2g_1 - g'_2, g_2) = G_\varepsilon^{-1/2}\mu^{\varepsilon/2}\underline{v}$ with $\underline{v} = (-2u_1 - u'_2, u_2)$ together with its bare form $\mathring{\underline{f}}$, define $\mathring{\gamma} = Z^{1/2}\gamma$, and compare the renormalizations, e.g.,

$$\begin{aligned} Z\mathring{\tau}' &= \underline{\underline{Z}} \cdot \underline{\tau}' = \underline{\underline{Z}} \cdot (\underline{\tau} + \gamma\,\underline{f}) \\ &= Z(\mathring{\underline{\tau}} + \mathring{\gamma}\,\mathring{\underline{f}}) \\ &= \underline{\underline{Z}} \cdot \underline{\tau} + \gamma G_\varepsilon^{-1/2}\mu^{\varepsilon/2}(\underline{v} + \underline{V}), \end{aligned} \tag{3.12}$$

where we have defined $\underline{V} = (-2B_1 - B'_2, B_2)$. It follows the Ward identity

$$(\underline{\underline{Z}} - \underline{\underline{1}}) \cdot \underline{v} = \underline{V}. \tag{3.13}$$

In the same way, we derive a second Ward identity

$$(\underline{v} \cdot \underline{\underline{A}})_i = \delta_{2,i} - Z_{2,i}. \tag{3.14}$$

In particular, we have $B_2 = -\underline{v} \cdot \underline{\underline{A}} \cdot \underline{v}$. Both Ward identities are easily verified at one-loop order with the diagrammatic results given in Appendix B. They reduce higher-order calculations enormously and lead to important relations between renormalization group functions and critical exponents. Being linear relations between the counterterms, the Ward identities

hold for each term of the Laurent expansions, in particular for the residua

$$Z_{2,i}^{(1)} = -\underline{v}\cdot\underline{\underline{A}}^{(1)}, \tag{3.15a}$$

$$\underline{V}^{(1)} = \underline{\underline{Z}}^{(1)}\cdot\underline{v}, \tag{3.15b}$$

$$B_2^{(1)} = -\underline{v}\cdot\underline{\underline{A}}^{(1)}\cdot\underline{v}. \tag{3.15c}$$

It is of some interest to state the Ward identities also in terms of the vertex functions. The shift invariance leads to the following identity for the vertex-function-generating functional (remember that no renormalizations are influenced by the shift):

$$\begin{aligned}\Gamma[\tilde\varphi,\varphi;\underline{\tau},h] &= \Gamma[\tilde\varphi,\varphi;\underline{\tau}] + (h,\tilde\varphi)\\ &= \Gamma\left[\tilde\varphi,\varphi+\gamma;\underline{\tau}+\underline{f}\gamma,h-\tau\gamma-\frac{g_2}{2}\gamma^2\right].\end{aligned} \tag{3.16}$$

Differentiation with respect to γ leads to the Ward identities

$$\Gamma_{\tilde k,k+1}(\{\mathbf{q}=0\}) = \tau\delta_{\tilde k,1}\delta_{k,0} - \underline{f}\cdot\frac{\partial}{\partial\underline{\tau}}\Gamma_{\tilde k,k}(\{\mathbf{q}=0\}) \tag{3.17}$$

between the vertex functions.

C. RG functions

RG functions express the change of the renormalized quantities under an infinitesimal change of the momentum scale μ (while holding bare quantities constant). They are the essential ingredients of the RG equations. As a scale change between two renormalized and therefore finite theories, the RG functions are themselves finite quantities without ε poles. We define

$$\beta_\alpha = \mu\partial_\mu u_\alpha\big|_0 = -\frac{\varepsilon}{2}u_\alpha + \beta_\alpha^{(0)}, \tag{3.18a}$$

$$\gamma = \mu\partial_\mu \ln Z\big|_0, \tag{3.18b}$$

where $\beta_\alpha^{(0)}$ and γ are independent of ε in minimal renormalization. It follows that

$$\mu\partial_\mu\big|_0 (Z,K,\ldots) = -\tfrac{1}{2}u\cdot\partial_u(Z^{(1)},K^{(1)},\ldots) + O(\varepsilon^{-1}), \tag{3.19}$$

where we abbreviate $\sum_\alpha u_\alpha\partial_{u_\alpha} =: u\cdot\partial_u$. Expanding in the following all expressions in Laurent series with respect to ε, and making use of the fact that all renormalized quantities are free of ε poles, we obtain

$$\beta_\alpha^{(0)} = \tfrac{3}{2}\gamma u_\alpha - \tfrac{1}{2}(1-u\cdot\partial_u)B_\alpha^{(1)}, \tag{3.20a}$$

$$\gamma = -\tfrac{1}{2}u\cdot\partial_u Z^{(1)}, \tag{3.20b}$$

$$\hat\gamma' = -\tfrac{1}{2}u\cdot\partial_u K^{(1)}, \tag{3.20c}$$

so that

$$\mu\partial_\mu|_0\tilde\varphi = -\tfrac{\gamma}{2}\tilde\varphi, \tag{3.21a}$$

$$\mu\partial_\mu|_0\varphi = -\tfrac{\gamma}{2}\varphi - \hat\gamma'\tilde\varphi \tag{3.21b}$$

in Green's functions. Similarly, we get

$$\mu\partial_\mu|_0\underline{\tau} = \underline{\tau}\cdot\underline{\underline{\hat\kappa}}, \tag{3.22a}$$

$$\mu\partial_\mu|_0 h = \frac{\gamma}{2}h + \frac{1}{2}G_\varepsilon^{1/2}\mu^{-\varepsilon/2}(\underline{\tau}\cdot\underline{\underline{\hat\alpha}}\cdot\underline{\tau}), \tag{3.22b}$$

where we have defined

$$\underline{\underline{\hat\kappa}} = \gamma\underline{\underline{1}} + \tfrac{1}{2}u\cdot\partial_u(\underline{\underline{Z}}^{(1)})^T, \tag{3.23a}$$

$$\underline{\underline{\hat\alpha}} = \tfrac{1}{2}(1+u\cdot\partial_u)\underline{\underline{A}}^{(1)}. \tag{3.23b}$$

It is now easy to derive relations between the Gell-Mann-Low functions with the help of the Ward identities (3.15). We obtain

$$\hat\kappa_{i,2} = \gamma\delta_{i,2} - (\underline{\underline{\hat\alpha}}\cdot\underline{v})_i, \tag{3.24a}$$

$$\underline{\hat\beta} = \tfrac{\gamma-\varepsilon}{2}\underline{v} + \underline{v}\cdot\underline{\underline{\hat\kappa}}, \tag{3.24b}$$

$$\hat\beta_2 = \tfrac{3\gamma-\varepsilon}{2}u_2 - \underline{v}\cdot\underline{\underline{\hat\alpha}}\cdot\underline{v}. \tag{3.24c}$$

Here we used the two-dimensional vectors $\underline{v} = (-2u_1 - u_2', u_2)$ and $\underline{\hat\beta} = (-2\beta_1 - \beta_2', \beta_2)$. In Appendix B, we state all the RG functions to one-loop order. With the results given there, the relations (3.24) are verified easily.

D. RG equations

Now, we derive the RG equations that determine how the quantities featured in our theory transform or flow under variation of the momentum scale μ. In order for the RG equations to produce reliable results, we have to remove at this stage any remaining scaling redundancy that could contaminate the RG flow. For example, if we continued using the variables of Sec. III C, we were at risk to erroneously conclude from Eq. (3.24b) that there is an eigenvalue $(\varepsilon-\gamma_*)/2$ of the matrix $\underline{\underline{\hat\kappa}}_*$ at a fixed point $(u_\alpha)_*$ with $\underline{\hat\beta}_* = 0$.

To remove the one remaining scaling redundancy from our theory, we switch to rescaling-invariant fields

$$\phi = u_2\varphi, \quad \tilde\phi = u_2^{-1}\tilde\varphi, \tag{3.25}$$

control parameters $\underline{t} = (\sigma,\tau)$ with

$$\sigma = u_2^2\rho, \tag{3.26a}$$

$$H = 2g_2 h, \tag{3.26b}$$

and the dimensionless coupling constants given by Eqs. (3.9). This procedure yields the new β functions:

$$\beta_u = u_2\beta_2' + u_2'\beta_2, \tag{3.27a}$$

$$\beta_v = u_2\beta_1 + u_1\beta_2, \tag{3.27b}$$

$$\beta_w = u_2^3\beta_0 + 3u_0u_2^2\beta_2. \tag{3.27c}$$

The Gell-Mann-Low functions designated with a hat change to

$$\gamma' = u_2^2\hat\gamma', \tag{3.28a}$$

$$\kappa_{1,1} = \hat\kappa_{1,1} + \zeta, \quad \kappa_{1,2} = u_2^{-2}\hat\kappa_{1,2}, \tag{3.28b}$$

$$\kappa_{2,1} = u_2^2\hat\kappa_{2,1}, \quad \kappa_{2,2} = \hat\kappa_{2,2}, \tag{3.28c}$$

$$\alpha_{1,1} = u_2^{-3}\hat\alpha_{1,1}, \quad \alpha_{1,2} = u_2^{-1}\hat\alpha_{1,2}, \quad \alpha_{2,2} = u_2\hat\alpha_{2,2}, \tag{3.28d}$$

where we have defined

$$\zeta = \frac{\beta_u}{u} = 2\frac{\beta_2}{u_2} = 2\frac{\beta_2'}{u_2'}. \tag{3.29}$$

Note that in case of $u = 0$, the function ζ is in general finite and nonzero.

Now, we are in the position to set up our ultimate RG equations. The generator $\mathcal{D}_\mu$ of the RG, i.e., the derivative $\mu\partial_\mu|_0$ purely expressed in terms of renormalized parameters, is given by

$$\mathcal{D}_\mu = \mu\frac{\partial}{\partial\mu} + \underline{t}\cdot\underline{\underline{\kappa}}\cdot\frac{\partial}{\partial\underline{t}} + \beta_u\frac{\partial}{\partial u} + \beta_v\frac{\partial}{\partial v} + \beta_w\frac{\partial}{\partial w}. \tag{3.30}$$

Its application to the fields in a correlation function produces the RG equations

$$\mathcal{D}_\mu\tilde{\phi} = -\frac{\gamma+\zeta}{2}\tilde{\phi}, \quad \mathcal{D}_\mu\phi = -\frac{\gamma-\zeta}{2}\phi - \gamma'\tilde{\phi}. \tag{3.31a}$$

In addition the RG equations of the external field H, which is linearly related to z (the integration variable of the inverse Laplace transformation), and the control parameters $\underline{t}$ are

$$\mathcal{D}_\mu H = \frac{\gamma+\zeta+\varepsilon}{2}H + \underline{t}\cdot\underline{\underline{\alpha}}\cdot\underline{t}, \tag{3.32a}$$

$$\mathcal{D}_\mu\underline{t} = \underline{t}\cdot\underline{\underline{\kappa}}. \tag{3.32b}$$

We introduce the combination

$$a = u + 2v = -v_1v_2, \tag{3.33}$$

with the corresponding Gell-Mann-Low function $\beta_a = \beta_u + 2\beta_v$ and the two-dimensional orthogonal vectors

$$\underline{w} = (a^{-1},1), \quad \overline{\underline{w}} = (-a,1). \tag{3.34}$$

The Ward identities (3.24) yield

$$\kappa_{i2} = \gamma\delta_{i,2} - (\overline{\underline{w}}\cdot\underline{\underline{\alpha}})_i \tag{3.35}$$

and the important relations between RG functions

$$(\overline{\underline{w}}\cdot\underline{\underline{\kappa}})_2 = (\varepsilon-\gamma+\zeta)/2, \tag{3.36a}$$

$$a^{-1}\beta_a = -\overline{\underline{w}}\cdot\underline{\underline{\kappa}}\cdot\underline{w}. \tag{3.36b}$$

The last equation in combination with the orthogonality of $\overline{\underline{w}}$ and $\underline{w}$ shows that these vectors are for $\beta_a = 0$ right and left eigenvectors of $\underline{\underline{\kappa}}$, respectively, with eigenvalues

$$\kappa_1 = (\underline{\underline{\kappa}}\cdot\underline{w})_2 = a(\underline{\underline{\kappa}}\cdot\underline{w})_1 - a^{-1}\beta_a, \tag{3.37a}$$

$$\kappa_2 = (\overline{\underline{w}}\cdot\underline{\underline{\kappa}})_2 = (\varepsilon-\gamma+\zeta)/2. \tag{3.37b}$$

Note that $\kappa_2 = (\varepsilon+\zeta-\gamma)/2$ determines the RG flow of the order-parameter field ϕ [Eq. (3.31a)]. This shows that each control parameter combination proportional to $\overline{\underline{w}}$ is redundant and can be eliminated by an order-parameter shift. Otherwise, the combination

$$y := \underline{t}\cdot\underline{w} = a^{-1}\sigma + \tau \tag{3.38}$$

is free of the shift redundancy and has the the independent scaling exponent κ_1. We expect that y defines the distance from the collapse transition line in the phase diagram.

To one-loop order, our diagrammatic calculation leads to

$$\beta_u = \Big(-\varepsilon+\frac{7}{2}u+10v\Big)u, \tag{3.39a}$$

$$\beta_v = \Big(-\varepsilon+\frac{25}{6}u+\frac{21}{2}v\Big)v - \frac{5}{6}w, \tag{3.39b}$$

$$\beta_w = \Big(-2\varepsilon+\frac{21}{2}u+25v\Big)w - \Big(5u^2+\frac{29}{2}uv+11v^2\Big)v, \tag{3.39c}$$

$$\gamma = -\frac{u+4v}{6}, \quad \gamma' = \frac{2uv+3v^2-w}{6}, \tag{3.39d}$$

and the matrices

$$\underline{\underline{\kappa}} = \begin{pmatrix} 8(2u+5v)/3-\varepsilon, & -1 \\ 5(w-2uv-3v^2)/3, & 5(u+4v)/6 \end{pmatrix}, \tag{3.40a}$$

$$\underline{\underline{\alpha}} = \begin{pmatrix} 0, & 1 \\ 1, & -2v \end{pmatrix}. \tag{3.40b}$$

With these one-loop results, the general results (3.35), (3.36), and (3.37), which hold to all loop orders, are easily verified.

E. RG flow and fixed points

The fixed points of our RG are determined by the zeros of the Gell-Mann-Low RG functions for the three coupling constants as given in Eqs. (3.39a)–(3.39c). The picture of the topology of the fixed points, invariant lines, and separating surfaces resulting from the RG flow that arises from these equations in the three-dimensional space spanned by these coupling constants is sketched in Fig. 13. The BRS plane $u = 0$ (red) is an invariant plane of the flow equations (3.39a)–(3.39c) to all orders and divides the (u,v,w) space in two parts: the percolation part with $u > 0$ (blue, I) and the Yang-Lee part with $u < 0$ (green, I and II). The latter part is nonphysical for the branched polymer problem. The percolation line $v = w = 0$ is an invariant line for both signs of u. For $u > 0$ the flow goes to the percolation fixed point (P), whereas for $u < 0$ the flow tends to infinity. The Yang-Lee line (bold green line) with $a = b = 0$, where $a = u + 2v$ and $b = u^2 + 4w$, is also an invariant line for both signs of u. For $u < 0$ the flow goes to the Yang-Lee fixed point (YL), whereas for $u > 0$ the flow runs away to infinity. Altogether we have six fixed points, which are compiled in Table I to one-loop order. Besides the trivial Gaussian fixed point (G) we find in the BRS plane the stable collapse fixed point (C) and an instable fixed point (In2). This point lies on a separatrix in the BRS plane (bold red line) and is attracting on it. The flow of the part that contains C is, of course, attracting to C. The other part shows runaway flow. Turning to the percolation part of the (u,v,w) space, there is the aforementioned instable percolation fixed point P on the percolation line $v = w = 0$. Because P has two stable directions, it defines a separating invariant surface with P as an attracting fixed point that divides the space in two parts. The flow in one of it goes to C, whereas the flow in the other part is again running away. The separating surface, the stability plane of P for $u > 0$, is a continuation of the separatrix found above on the BRS plane for $u = 0$. In the Yang-Lee part of the (u,v,w) space, we also find a separating surface that is the continuation of the BRS separatrix now into the region with

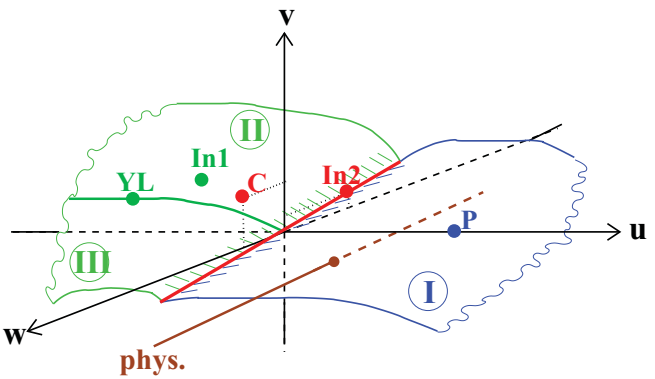

FIG. 13. (Color online) Sketch of the invariant manifolds of the RG flow as explained in the text.

$u < 0$. This invariant surface is separated in two parts by the Yang-Lee line. One part is attracting to an instable fixed point (In1); the other part shows runaway flow. Both surfaces divide the (u,v,w) space in a wedge-shaped part attracting to C, and a part where the flow goes to infinity. The edge of the wedge is the separatrix in the BRS plane. Note that the two separating surfaces are not smoothly connected at the separatrix since the BRS plane is itself a separating surface.

The line labeled phys. (brown) is closely related to the collapse line in the phase diagram (Fig. 1), and its meaning is as follows. Recall that we focus on asymptotically large RBPs, and hence the external field h is near criticality. The control parameter y and the three coupling constants are thought to be expressed as functions of the two fugacities spanning the phase diagram. At the collapse, i.e., when y becomes critical, the two fugacities are not independent, and hence, the coupling constants can be parametrized in terms of a single fugacity. Hence the collapse line in the phase diagram corresponds to a line in the flow diagram, which we represent by the brown line. As long as this line lies above the percolation surface, the RG flows to C. From the point where the brown line pierces the blue percolation surface, the RG flows to the percolation fixed point P. From any point on the line below the percolation surface, the RG runs off to infinity.

Before returning to the θ transition as our main focus, we would like point out the following lesson regarding the θ' transition that our flow diagram teaches. Usually runaway flows are associated with fluctuation-induced first-order transitions. Here the region below the percolation surface where the coupling constants runs away to ever more positive values indicates that this transition might be discontinuous and not, as previously assumed, a second-order transition.

TABLE I. RG fixed points to leading order.

	u_*	v_*	w_*	Stability
G	0	0	0	− − −
C	0	$\frac{\varepsilon(69+\sqrt{201})}{760}$	$\frac{6\varepsilon^2(689\sqrt{201}-339)}{5\times 760^2}$	+ + +
P	$\frac{2\varepsilon}{7}$	0	0	+ + −
YL	$-\frac{2\varepsilon}{3}$	$\varepsilon/3$	$-\varepsilon^2/9$	+ − −
In1	$-\frac{\varepsilon}{2}$	$11\varepsilon/40$	$-517\varepsilon^2/8000$	+ + −
In2	0	$\frac{\varepsilon(69-\sqrt{201})}{760}$	$\frac{-6\varepsilon^2(689\sqrt{201}+339)}{5\times 760^2}$	+ − −

F. Scaling at the collapse transition

Now, we determine the scaling behavior of the order parameter $\langle\tilde{n}\rangle_z = \langle\varphi\rangle_z = \Phi/g_2$ (here we have included a factor g_2 in the definition of Φ for convenience), the correlation function of φ and $\tilde{\varphi}$, and the correlation length. The external field $H = 2g_2h$ (which is a linear function of the Laplace variable z) is related to Φ via the equation of state

$$h + \left.\frac{\delta\Gamma[\tilde{\varphi},\varphi;\underline{\tau}]}{\delta\tilde{\varphi}}\right|_{\tilde{\varphi}=0,\varphi=\Phi/g_2} = 0, \tag{3.41}$$

where $\Gamma[\tilde{\varphi},\varphi;\underline{\tau}]$ is the vertex-generating functional. The equation of state guarantees that tadpole insertions in diagrams are canceled by the external field h, and $\langle\varphi\rangle = 0$ after the shift $\varphi \to \varphi + \Phi/g_2$. Using again the shift symmetry of the vertex-generating function [Eq. (3.16)], the equation of state (3.41) is reduced to

$$H + \tau^2 = (\tau - \Phi)^2 + T(\sigma + a\Phi, \tau - \Phi), \tag{3.42}$$

where $T(\underline{t}) = -2g_2\Gamma_{1,0}(\underline{\tau})$ is the sum of the tadpole diagrams, which we have calculated to one-loop order. To find Φ as a function of z, we invert Eq. (3.42) and obtain $(\tau - \Phi)$ as a function of $(H + \tau^2)$ and y. The inverse has according to Eq. (3.41) a critical point at a value of Φ where

$$g_2\frac{\partial}{\partial\Phi}\left(\left.\frac{\delta\Gamma[\tilde{\varphi},\varphi;\underline{\tau}]}{\delta\tilde{\varphi}}\right|_{\tilde{\varphi}=0,\varphi=\Phi/g_2}\right) = \Gamma_{1,1}(\mathbf{q}=0, \sigma + a\Phi, \tau - \Phi) = 0. \tag{3.43}$$

This condition determines eventually the critical value z_c of the inverse Laplace transformation, where the first singularity in the complex z plane is positioned. It is therefore the value where the correlation length $\xi(z) \sim 1/\sqrt{\Gamma_{1,1}(\mathbf{q}=0)}$ tends to infinity.

To find the scaling behavior of Φ as a function of $(z - z_c)$ near this critical point, we examine the RG flow of the shift-invariant combinations of control parameters $y = (\tau + a^{-1}\sigma)$, $M = (\tau - \Phi)$, and $L = (\tau^2 + H) \sim (z - z_c)$. Note that at this point the redundant variable τ can be set to zero. The RG equations for these combinations are easily derived from Eqs. (3.31a), (3.32a), and (3.32b) using the properties that follow from the Ward identities. They are given by

$$\mathcal{D}_\mu y = \kappa_1 y, \tag{3.44a}$$

$$\mathcal{D}_\mu M = \kappa_2 M + \kappa_{1,2} a y, \tag{3.44b}$$

$$\mathcal{D}_\mu L = (\kappa_2 + \gamma)L + \alpha_{1,1} a^2 y^2. \tag{3.44c}$$

The solutions of these flow equations at a fixed point in terms of a flow parameter l such that $\mu(l) = \mu l$ are given by

$$y(l) = l^{\kappa_{1*}} y, \tag{3.45a}$$

$$M(l) + p_1 y(l) = l^{\kappa_{2*}}(M + p_1 y), \tag{3.45b}$$

$$L(l) + p_2 y(l)^2 = l^{(\kappa_2+\gamma)_*}(L + p_2 y^2), \tag{3.45c}$$

where $p_1 = [\kappa_{1,2} a/(\kappa_2 - \kappa_1)]_*$ and $p_2 = [\alpha_{1,1} a^2/(\kappa_2 + \gamma - 2\kappa_1)]_*$. Taking into account the naive dimensions of M, y,

and L, the relation between these quantities as the inversion of Eq. (3.42) is

$$[M(l)+p_1 y(l)]/\mu(l)^2 = F\big([L(l)+p_2 y(l)^2]/\mu(l)^4, y(l)/\mu(l)^2\big) \quad (3.46)$$

in dimensionless form. Choosing l so that $(L(l)+p_2 y(l)^2)/\mu(l)^4 = 1$, we obtain the order-parameter equation in scaling form

$$M + p_1 y = (L + p_2 y^2)^{\beta/\Delta} \mathcal{F}[y/\big(L + p_2 y^2\big)^{1/\Delta}], \quad (3.47)$$

and setting $(L + p_2 y^2) \sim (z - z_c)$ and $(M + p_1 y) \sim (\Phi_c - \Phi)$, we obtain

$$\Phi_c - \Phi = (z - z_c)^{\beta/\Delta} \mathcal{F}_\Phi[y/(z - z_c)^{1/\Delta}]. \quad (3.48)$$

Here the scaling function $\mathcal{F}_\Phi$ is identical to $\mathcal{F}$ up to some noninteresting constant factors, and the critical exponents are given by the fixed point values of the various RG functions

$$1/\nu = 2 - \kappa_{1*}, \quad \eta = \gamma_* - \zeta_*, \quad \tilde{\eta} = \gamma_* + \zeta_*, \quad (3.49a)$$

$$\beta/\nu = 2 - \kappa_{2*} = \tfrac{1}{2}(d - 2 + \eta), \quad (3.49b)$$

$$\Delta/\nu = 4 - \kappa_{2*} - \gamma_* = \tfrac{1}{2}(d + 2 - \tilde{\eta}). \quad (3.49c)$$

If $\zeta_* \neq 0$, which happens if $u_* = 0$ and thus holds true at the collapse transition, we find three independent critical exponents η, $\tilde{\eta}$, and ν.

The RG equation for the correlation function $G_{1,1}(\mathbf{r}) = \langle \phi(\mathbf{r})\tilde{\phi}(\mathbf{0})\rangle_z^{(\mathrm{cum})}$ follows from Eq. (3.31a) as

$$(\mathcal{D}_\mu + \gamma_*) G_{1,1}(\mathbf{r}) = 0 \quad (3.50)$$

at a fixed point. Using again the flow parameter l, we obtain the solution

$$\begin{aligned} &G_{1,1}(\mathbf{r}, y, M + p_1 y, \mu) \\ &\quad = l^{\gamma_*} G_{1,1}[\mathbf{r}, l^{\kappa_{1*}} y, l^{\kappa_{2*}}(M + p_1 y), \mu l] \\ &\quad = l^{d-2+\gamma_*} G_{1,1}[l\mathbf{r}, y/l^{1/\nu}, (M + p_1 y)/l^{\beta/\nu}, \mu]. \end{aligned} \quad (3.51)$$

Taking y and $(z - z_c)$ as independent variables, and expressing $(M + p_1 y)$ through the equation of state (3.48), we find after choosing l as above the scaling form

$$G_{1,1}(\mathbf{r}, z) = \frac{\mathcal{G}_{1,1}[\mathbf{r}(z - z_c)^{\nu/\Delta}, y/(z - z_c)^{1/\Delta}]}{|\mathbf{r}|^{d-2+(\eta+\tilde{\eta})/2}}. \quad (3.52)$$

The correlation length ξ is defined by

$$\xi^2 = \frac{1}{2d} \int d^d r\, \mathbf{r}^2 G_{1,1}(\mathbf{r}) \Big/ \int d^d r\, G_{1,1}(\mathbf{r}) = \frac{\partial \ln \Gamma_{1,1}(\mathbf{q})}{\partial q^2}\bigg|_{\mathbf{q}=0}, \quad (3.53)$$

where the vertex function $\Gamma_{1,1}(\mathbf{r})$ is related to the Fourier-transformed correlation function by $\tilde{G}_{1,1}(\mathbf{q}) = 1/\Gamma_{1,1}(\mathbf{q})$. Hence the correlation length scales as

$$\xi(z) \sim (z - z_c)^{-\nu/\Delta}. \quad (3.54)$$

In terms of ξ, the correlation function is given by

$$G_{1,1}(\mathbf{r}, z) = \frac{\mathcal{G}_{1,1}(\mathbf{r}/\xi, y\xi^{1/\nu})}{|\mathbf{r}|^{d-2+(\eta+\tilde{\eta})/2}}. \quad (3.55)$$

TABLE II. Padé estimates of the critical exponents.

d	θ	ϕ	ν_{A}
2	1.96(4)	0.37(2)	0.52(3)
3	2.13(2)	0.427(5)	0.396(7)
4	2.277(5)	0.469(1)	0.329(2)
5	2.4025(6)	0.49383(2)	0.2849(2)
6	2.5	0.5	0.25

IV. OBSERVABLES OF THE COLLAPSING BRANCHED POLYMER

In this section we translate our RG results into a language that is more geared toward polymer physics. In particular, we extract the probability distribution $\mathcal{P}(N)$, the radius of gyration, and the shape function. As explained in detail in Sec. II, these kinds of quantities as functions of N are related to the quantities native to our field theory via inverse Laplace transformation.

A. Scaling behavior

The probability distribution $\mathcal{P}(N)$ is given by Eq. (2.23), and asymptotically for $N \gg 1$, we derive

$$\begin{aligned} \mathcal{P}(N) &\sim \mathrm{e}^{z_c N} \int_0^\infty dx\, \frac{\mathrm{Disc}\,\Phi(z_c - x)}{2\pi i} \mathrm{e}^{-xN} \\ &\sim \mathrm{e}^{z_c N} \int_0^\infty dx\, \frac{\mathrm{Disc}\{(-x)^{\beta/\Delta} \mathcal{F}_\Phi[y/(-x)^{1/\Delta}]\}}{2\pi i} \mathrm{e}^{-xN} \\ &\sim N^{-1-\beta/\Delta} \mathrm{e}^{z_c N} \\ &\quad \times \int_0^\infty dx'\, \frac{\mathrm{Disc}\{(-x)^{\beta/\Delta} \mathcal{F}_\Phi[N^{1/\Delta} y/(-x')^{1/\Delta}]\}}{2\pi i} \mathrm{e}^{-x'}. \end{aligned} \quad (4.1)$$

Hence, we immediately obtain the asymptotic scaling form of the animal numbers from Eq. (2.18) as

$$\mathcal{A}(N) \sim N^{-1} \mathcal{P}(N) \sim N^{-\theta} \kappa^N f_{\mathcal{A}}(y N^{\phi}), \quad (4.2)$$

where the animal exponent θ and the crossover exponent ϕ are given by

$$\theta = 2 + \beta/\Delta = 2 + \frac{d - 2 + \eta}{d + 2 - \tilde{\eta}}, \quad (4.3a)$$

$$\phi = \tfrac{1}{\Delta} = \frac{2}{\nu(d + 2 - \tilde{\eta})}. \quad (4.3b)$$

In the same way we find the scaling behavior of the monomer distribution of a collapsing branched polymer, which was calculated in mean-field theory in Eq. (2.32). Here we derive from the correlation function that (3.55)

$$\begin{aligned} G_N(\mathbf{r}) &= \frac{1}{\mathcal{P}(N)} \int_{\sigma - i\infty}^{\sigma + i\infty} \frac{dz}{2\pi i}\, \mathrm{e}^{zN} G_{1,1}(\mathbf{r}; z) \\ &= \frac{N^{\theta-1}}{|\mathbf{r}|^{d-2+(\eta+\tilde{\eta})/2}} \\ &\quad \times \int_0^\infty dx\, \frac{\mathrm{Disc}\,\mathcal{G}_{1,1}[\mathbf{r}(-x)^{\nu/\Delta}, y/(-x)^{1/\Delta}]}{2\pi i} \mathrm{e}^{-xN} \\ &= \frac{N^{\theta-1}}{|\mathbf{r}|^{d-2+(\eta+\tilde{\eta})/2}} G(\mathbf{r}/N^{\nu/\Delta}, y N^{1/\Delta}). \end{aligned} \quad (4.4)$$

Defining the radius of gyration R_N as in Eq. (2.34), we write the monomer distribution in the scaling form

$$G_N(\mathbf{r}) = \frac{N}{R_N^d}\mathcal{G}(|\mathbf{r}|/R_N, yN^\phi) \tag{4.5}$$

with the radius of gyration

$$R_N = N^{\nu_A}\mathcal{R}(yN^\phi). \tag{4.6}$$

Its exponent is given by

$$\nu_A = \nu/\Delta = \frac{2}{d+2-\tilde{\eta}}. \tag{4.7}$$

As it should, our result satisfies the sum rule

$$\int d^d x\, \mathcal{G}(\mathbf{x}, yN^\phi) = 1. \tag{4.8}$$

Next, we state our ε-expansion results for the exponents governing the collapse transition. Thus far, when it came to the diagrammatic part of our theory, we centered our discussion around the one-loop order of our calculation to keep matters as simple as possible. Our actual calculation, however, went to higher order, which allows us to present here results for the critical exponents of the θ transition to second order in ε. Details of this calculation will be presented elsewhere [37]. For completeness, we list in Appendix C our two-loop results for the RG functions that went into the calculation of the critical exponents. For the three independent exponents defined in Eqs. (4.3) and (4.7), we obtain

$$\theta = \tfrac{5}{2} - 0.4925\,(\varepsilon/6) - 0.5778\,(\varepsilon/6)^2, \tag{4.9a}$$

$$\phi = \tfrac{1}{2} + 0.0225\,(\varepsilon/6) - 0.3580\,(\varepsilon/6)^2, \tag{4.9b}$$

$$\nu_A = \tfrac{1}{4} + 0.1915\,(\varepsilon/6) + 0.0841\,(\varepsilon/6)^2. \tag{4.9c}$$

From these expansions, we derive numerical results of the exponents for dimensions 2 to 5 by performing simple Padé estimates [26,27] (see Table II).

For $d = 2$ dimensions, there exist numerical results to which our ε-expansion results can be compared. Simulations by Hsu and Grassberger [8] for the tree part of the collapse transition produce $\theta = 1.845$ and $\nu_A = 0.5362$. These results compare partially satisfactory within the expectations for such a big value of ε. To improve the agreement between our theoretical predictions and the simulations or potential experiments, it is desirable to extend our calculation to higher order [38] and apply more sophisticated resummation methods.

Next, we consider corrections to scaling. To determine the leading corrections, it is useful to distinguish between two phenomena. First, there is the irrelevance of cycles near the θ transition and the associated crossover to tree behavior with BRS symmetry. For this crossover, the coupling constant u is proportional to the cycle fugacity z_{cy}. Using the RG result $u(l) = ul^{\zeta_*}$ and choosing a small parameter l proportional to R_N^{-1}, we find that this crossover leads to a correction to all scaling functions proportional to u/N^{x_u}, where

$$x_u = \nu_A\zeta_* = d\nu_A + 1 - \Theta \tag{4.9d}$$

is the corresponding crossover exponent. Second, there is the approach of the coupling constants v and w to their fixed-point values. This approach is described by the eigenvalues of the matrix of first derivatives of the functions β_v and β_w, respectively,

$$\omega_1 = \varepsilon - 0.7614\,\varepsilon^2, \quad \omega_2 = 1.0344\,\varepsilon - 0.6830\,\varepsilon^2. \tag{4.9e}$$

These so-called Wegner exponents lead to corrections proportional to N^{-x_i} with $x_i = \nu_A\omega_i$.

B. The shape of the collapsing branched polymer

Here we will derive the asymptotic forms of the shape function $\mathcal{G}(\mathbf{r}/R_N, yN^\phi)$ [Eq. (4.5)] of the monomer distribution for small and large $|\mathbf{r}|/R_N$ at the collapse transition line $y = 0$. We use methods analogous to methods applied in Refs. [39–41] to the case of linear polymers.

In a first and somewhat hand-waving approach, we assume that the monomer distribution in the interior of the branched polymer is independent of the size N. Hence, for $x \to 0$, we should have

$$\mathcal{G}(x,0) \sim x^{-d+1/\nu_A}, \tag{4.10}$$

leading to the monomer distribution for $|\mathbf{r}| \ll R_N$

$$G_N(\mathbf{r}) \sim \frac{1}{|\mathbf{r}|^{d-1/\nu_A}}. \tag{4.11}$$

Next, we derive this result more rigorously by application of the short distance expansion. The leading terms of the operator product expansions are given by

$$\tilde{\phi}(\mathbf{r}+\mathbf{x}/2)\tilde{\phi}(\mathbf{r}-\mathbf{x}/2) = c_1(\mathbf{x},\mu)\tilde{\phi}(\mathbf{r}), \tag{4.12a}$$

$$\phi(\mathbf{r}+\mathbf{x}/2)\tilde{\phi}(\mathbf{r}-\mathbf{x}/2) = c_2(\mathbf{x},\mu)\tilde{\phi}(\mathbf{r}) + c_3(\mathbf{x},\mu)\phi(\mathbf{r}), \tag{4.12b}$$

$$\phi(\mathbf{r}+\mathbf{x}/2)\phi(\mathbf{r}-\mathbf{x}/2) = c_4(\mathbf{x},\mu)\tilde{\phi}(\mathbf{r}) + c_5(\mathbf{x},\mu)\phi(\mathbf{r}). \tag{4.12c}$$

The form of these expansions is dictated by the symmetry of our model: $\tilde{\varphi}$ belongs to the trivial representation of the permutation group $S_{n\to 0}$, and φ has components belonging to the trivial and the fundamental representation. The scaling behavior of the functions $c_i(\mathbf{x},\mu) \sim \mu^{(d-2)/2}$ follows from the RGE. Applying the RG differential $\mathcal{D}_\mu$ operator to both sides of (4.12) and comparing the results, we find

$$\mathcal{D}_\mu c_{1,3}(\mathbf{x},\mu) = -\frac{\tilde{\eta}}{2}c_{1,3}(\mathbf{x},\mu) \tag{4.13}$$

at the collapse fixed point. Hence

$$\begin{aligned} c_{1,3}(\mathbf{x},\mu) &= l^{\tilde{\eta}/2}c_{1,3}(\mathbf{x},l\mu) \\ &= (l\mu)^{(d-2)/2}l^{\tilde{\eta}/2}c_{1,3}(l\mu\mathbf{x},1) = \frac{c_{1,3}(1,1)}{\mu^{\tilde{\eta}/2}\,|\mathbf{x}|^{d-1/\nu_A}}. \end{aligned} \tag{4.14}$$

Using Eq. (4.12b), we obtain

$$G_{1,1}(\mathbf{r};z) \sim \frac{\Phi(z)}{|\mathbf{r}|^{d-1/\nu_A}}. \tag{4.15}$$

This argument has to be taken with a grain of salt. Strictly speaking, the operator product expansion has to be inserted in Green's functions that are superficially convergent; otherwise

one has to deal with additive renormalizations. Therefore $G_{1,1}(\mathbf{r};z)$ in Eq. (4.15) is determined only up to a polynomial in z. However, this polynomial is canceled by the inverse Laplace transformation as long as $N > 0$. Hence, after the application of the inverse Laplace transformation to Eq. (4.15) and division by $\mathcal{P}(N)$, we indeed get the result stated in Eq. (4.11).

Now we turn to the large $|\mathbf{r}|$ (or small $|\mathbf{q}|$) behavior of the correlation function. In this regime, the appropriate vertex function is well approximated by

$$\Gamma_{1,1}(\mathbf{q},z) \approx \Gamma_{1,1}(\mathbf{0},z)[1+\xi(z)^2\mathbf{q}^2], \tag{4.16a}$$

$$\Gamma_{1,1}(\mathbf{0},z) \sim \xi(z)^{-2+(\eta+\tilde{\eta})/2}. \tag{4.16b}$$

The correlation function has the representation

$$G_{1,1}(\mathbf{r};z) \sim \xi(z)^{-(\eta+\tilde{\eta})/2} \int_0^\infty ds\ \exp[-\xi(z)^{-2}s - \mathbf{r}^2/4s]. \tag{4.17}$$

Taking the conditions $\mathbf{r}^2/\xi(z)^2 \gg 1$, $N \gg 1$ into consideration, we calculate the monomer distribution employing a double saddle-point approximation of the s and z integral. We find the distribution in the form of Eq. (4.5) with the shape function

$$\mathcal{G}(x,0) \sim x^{-t} \exp(-cx^{1/(1-\nu_A)}). \tag{4.18}$$

Here c is a constant, and the exponent is

$$t = d - \frac{d/2 - 2 + \theta}{1-\nu_A}. \tag{4.19}$$

C. Fractal dimensions

We conclude this section by briefly discussing the fractal dimensions associated with RBPs. As discussed on several occasions in this paper, collapsing RBPs have a treelike structure; i.e., they are quasi-one-dimensional. Thus, the dimension $d_{\min}$ of the shortest path between two points on the polymer, also known as the chemical distance, the backbone dimension d_{bb}, and the resistor dimension d_{rr} coincide. The fractal dimension d_f governing the total mass of the RBP is $d_f = 1/\nu_A$, and the exponent for random walks on a RPB is given by $d_w = d_{\min} + d_f$. From what we have presented thus far in this paper, we know d_f to two-loop order. Knowing the other fractal dimensions requires to calculate $d_{\min}$, which is identical to the dynamical exponent z of our model. This calculation is beyond the scope of this paper and will be presented elsewhere [37]. For completeness, however, we find it useful to mention here the results of our dynamical calculation. For the θ transition, we find

$$d_{\min} = 2 - 0.8756\,(\varepsilon/6) - 1.1528\,(\varepsilon/6)^2. \tag{4.20}$$

For the swollen RPBs, we obtain

$$d_{\min} = 2 - (\varepsilon/9) - \tfrac{35}{18}\,(\varepsilon/9)^2, \tag{4.21}$$

where $\varepsilon = 8 - d$ because $d = 8$ is the upper critical dimension for the swollen phase. Padé estimates are given in Table III.

TABLE III. Padé estimates of the minimal dimension.

d	$d_{\min}$ (swollen)	$d_{\min}$ (collapse)
2	1.09	1.21
3	1.22	1.415
4	1.37	1.624
5	1.536	1.8277
6	1.707	2
7	1.868	2
8	2	2

V. CONCLUDING REMARKS AND OUTLOOK

In summary, we developed a new, dynamical field theory for isotropic randomly branched polymers, and we used this model in conjunction with the RG to take a fresh look at this classical problem of statistical physics. We demonstrated that our model provides an alternative vantage point to understand the swollen phase via dimensional reduction. We corrected and pushed ahead the critical exponents for the θ transition. We showed that at the stable fixed point the model has BRS symmetry. Hence, asymptotically the RBPs are dominated by tree configurations. Our RG analysis produces evidence for the θ' transition being a fluctuation induced first-order transition and not as previously assumed a second-order transition. It would be interesting to see if future experimental or numerical studies can confirm the latter finding.

Complementary to the quasistatic RG analysis presented in this paper, we have also conducted a field theoretic calculation of the dynamical exponent z of our dynamical model [37]. This calculation produced the first-ever field theoretic results, quoted above, for the fractal dimension $d_{\min}$ of the shortest path and related fractal dimensions for RBPs. We are currently completing a three-loop calculation of the asymmetric Potts model. This calculation pushes the exponents θ, ϕ, and ν_A to third order in ε [38].

APPENDIX A: THE QUASISTATIC LIMIT

This appendix provides background on the quasistatic limit that we invoke in Sec. II in the derivation of our field theoretic Hamiltonian. Let us consider a dynamic response functional of the general form

$$\mathcal{J}[\tilde{n},n] = \int d^dx dt \lambda\tilde{n}[\lambda^{-1}\partial_t + \tau - \nabla^2]n + \mathcal{W}[\tilde{n},n], \tag{A1}$$

where the interaction part $\mathcal{W}$ reduces to a time-independent functional $\overline{\mathcal{W}}[\tilde{n}_0,m_\infty]$ of $\tilde{n}_0(\mathbf{r})$ and $m_\infty(\mathbf{r}) = \lambda\int_{-\infty}^{+\infty} dt n(\mathbf{r},t)$ after setting $\tilde{n}(\mathbf{r},t) \to \tilde{n}_0(\mathbf{r}) = \tilde{n}(\mathbf{r},0)$. We define

$$\mathcal{H}_{qs}[\tilde{n}_0,m_\infty] := \mathcal{J}[\tilde{n}_0,n] = \int d^dx \tilde{n}_0[\tau - \nabla^2]m_\infty + \overline{\mathcal{W}}[\tilde{n}_0,m_\infty], \tag{A2}$$

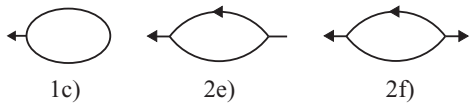

FIG. 14. One-loop diagrams with a correlator.

where $\mathcal{H}_{qs}$ denotes the quasistatic Hamiltonian. The free causal propagator

$$G(\mathbf{r}-\mathbf{r}',t-t') = \langle n(\mathbf{r},t)\tilde{n}(\mathbf{r}',t')\rangle_0 \sim \theta(t-t') \tag{A3}$$

with $\theta(t)=1$ if $t>0$ and $\theta(t)=0$ if $t\leqslant 0$ becomes the static propagator of $\mathcal{H}_{qs}$ after time integration

$$\begin{aligned}\lambda\int_{-\infty}^{\infty} dt\,\langle n(\mathbf{r},t)\tilde{n}(\mathbf{r}',t')\rangle_0 &= \lambda\int_0^{\infty} dt\,\langle n(\mathbf{r},t)\tilde{n}(\mathbf{r}',0)\rangle_0 \\ &= \langle m_\infty(\mathbf{r})\tilde{n}_0(\mathbf{r}')\rangle_0 = G_{st}(\mathbf{r}-\mathbf{r}').\end{aligned} \tag{A4}$$

Now consider a diagram of the graphical perturbation expansion of the connected correlation function $\langle\prod_i m_\infty(\mathbf{r}_i)\prod_j \tilde{n}(\mathbf{r}_j,0)\rangle$. By causality, the vertices of the diagram are ordered in time from "left" (i.e., the largest time involved) to "right" (the smallest time); $\tilde{n}$ legs are left-going, n legs are right-going. Consider the first vertex, which has only propagators (we suppress the space arguments) $\langle m_\infty\tilde{n}(t_1)\rangle_0 = \langle m_\infty\tilde{n}_0\rangle_0$ on its $\tilde{n}$ legs. Hence, the time dependence of the $\tilde{n}$ legs of this vertex is absorbed by the m_∞, each $\tilde{n}(t_1)$ becomes a time-independent $\tilde{n}_0$, and after integration over the vertex time t_1, the integrated vertex becomes a vertex generated by the quasistatic interaction $\overline{\mathcal{W}}[\tilde{n}_0,m_\infty]$. By induction, one can prove that this mechanism carries through all the way to and including the last vertex. The full diagram is therefore generated only by static propagators and the interaction vertices of the quasistatic Hamiltonian $\mathcal{H}_{qs}[\tilde{n}_0,m_\infty]$. By itself, however, the quasistatic Hamiltonian is insufficient to describe the static properties of the theory. As a remnant of its dynamical origin, $\mathcal{H}_{qs}$ must be supplemented with the causality rule that forbids the former time-closed propagator loops. Hence the terminology *quasi*static.

APPENDIX B: ONE-LOOP PERTURBATION THEORY

In this Appendix we assemble and list our results for the superficially diverging vertex functions $\Gamma_{1,0}$, $\Gamma_{1,1}$, $\Gamma_{2,0}$, $\Gamma_{1,2}$, $\Gamma_{2,1}$, and $\Gamma_{3,0}$ in the case $\rho=0$. Recall that we have already calculated the decorations of the diagrams contributing to these vertex functions in Sec. II. Thus it remains to perform the integrations over the internal momenta of these diagrams. There are three types of integrals appearing:

$$I_1(\tau) = \int_{\mathbf{p}} \frac{1}{\tau+\mathbf{p}^2} = \frac{G_\varepsilon \tau^{2-\varepsilon/2}}{(1-\varepsilon/4)(1-\varepsilon/2)\varepsilon}, \tag{B1}$$

$$\begin{aligned}I_2(\tau,\mathbf{q}) &= \int_{\mathbf{p}} \frac{1}{(\tau+\mathbf{p}^2)[\tau+(\mathbf{p}+\mathbf{q})^2]} \\ &= -\frac{2G_\varepsilon\tau^{1-\varepsilon/2}}{(1-\varepsilon/2)\varepsilon} - \frac{(1-\varepsilon/4)G_\varepsilon\tau^{-\varepsilon/2}}{3(1-\varepsilon/6)\varepsilon}\mathbf{q}^2,\end{aligned} \tag{B2}$$

$$I_3(\tau) = \int_{\mathbf{p}} \frac{1}{(\tau+\mathbf{p}^2)^3} = \frac{G_\varepsilon\tau^{-\varepsilon/2}}{\varepsilon}, \tag{B3}$$

where we have dropped the UV convergent parts of the integrals, which are unimportant for our purposes. In addition to the ($\rho=0$) diagrams listed in Sec. II, we need a few more diagrams that determine the renormalization of ρ. Those are the diagrams with an insertion of a ρ vertex, or in other words, diagrams where a propagator is replaced by a correlator; see Fig. 14. These diagrams can be expressed as

$$1c) = -\frac{g_2}{2}\rho I_2(\tau,\mathbf{0}), \tag{B4}$$

$$2e) = -g_2^2\rho I_3(\tau), \tag{B5}$$

$$2f) = 2g_2(2g_1+g_2')\rho I_3(\tau). \tag{B6}$$

Altogether we obtain the ε-pole contributions

$$\Gamma_{1,0} = h-(1b)-(1c) = h+\frac{G_\varepsilon\tau^{-\varepsilon/2}}{\varepsilon}(g_1\tau^2-g_2\tau\rho), \tag{B7}$$

$$\begin{aligned}\Gamma_{1,1} &= (\tau+\mathbf{q}^2)-(2b)-(2e) \\ &= \left\{\tau-\frac{G_\varepsilon\tau^{-\varepsilon/2}}{\varepsilon}[g_2(4g_1+g_2')\tau-g_2^2\rho]\right\} \\ &\quad +\left[1-\frac{G_\varepsilon\tau^{-\varepsilon/2}}{6\varepsilon}g_2(4g_1+g_2')\right]\mathbf{q}^2,\end{aligned} \tag{B8}$$

$$\begin{aligned}\Gamma_{2,0} &= \rho-(2c)-(2f) \\ &= \left\{\rho-2\frac{G_\varepsilon\tau^{-\varepsilon/2}}{\varepsilon}\big[\big(g_0g_2-3g_1^2-2g_1g_2'\big)\tau\right. \\ &\quad \left.+(2g_1g_2+g_2g_2')\rho\big]\right\} \\ &\quad +\left[1-\frac{G_\varepsilon\tau^{-\varepsilon/2}}{3\varepsilon}\big(g_0g_2-3g_1^2-2g_1g_2'\big)\right]\mathbf{q}^2,\end{aligned} \tag{B9}$$

$$\begin{aligned}\Gamma_{1,2} &= -g_2-(3b) \\ &= -\left[1-2\frac{G_\varepsilon\tau^{-\varepsilon/2}}{\varepsilon}(3g_1g_2+g_2g_2')\right]g_2,\end{aligned} \tag{B10}$$

$$\begin{aligned}\Gamma_{2,1} &= (2g_1+g_2')-(3c) \\ &= 2g_1-2\frac{G_\varepsilon\tau^{-\varepsilon/2}}{\varepsilon}[(7g_1g_2+3g_2g_2')g_1-g_2g_0] \\ &\quad +\left[1-2\frac{G_\varepsilon\tau^{-\varepsilon/2}}{\varepsilon}(3g_1g_2+g_2g_2')\right]g_2',\end{aligned} \tag{B11}$$

$$\begin{aligned}\Gamma_{3,0} &= g_0-(3d) \\ &= g_0-2\frac{G_\varepsilon\tau^{-\varepsilon/2}}{\varepsilon}\big[3\big(2g_1g_2+g_2g_2'\big)g_0 \\ &\quad -\big(7g_1^2+9g_1g_2'+3g_2'^2\big)g_1\big].\end{aligned} \tag{B12}$$

where all quantities, vertex functions, control parameters, and couplings are bare quantities. Recall from the main text that we switch notation when we apply our renormalization scheme in that we put an overcirc over bare quantities, e.g., $\Gamma_{1,0}\to\mathring{\Gamma}_{1,0}$, and we understand quantities without an overcirc as renormalized ones once the renormalization scheme has

been applied. Keeping this in mind when we compare the vertex-generating function in its bare and renormalized forms,

$$\Gamma = \sum_{\tilde{k},k} \mathring{\Gamma}_{\tilde{k},k} \frac{\mathring{\tilde{\varphi}}^{\tilde{k}} \mathring{\varphi}^{k}}{\tilde{k}!k!} = \sum_{\tilde{k},k} \Gamma_{\tilde{k},k} \frac{\tilde{\varphi}^{\tilde{k}} \varphi^{k}}{\tilde{k}!k!}, \tag{B13}$$

we obtain the following renormalizations of the vertex functions:

$$\Gamma_{1,0} = Z^{1/2} \mathring{\Gamma}_{1,0}, \tag{B14}$$

$$\Gamma_{1,1} = Z \mathring{\Gamma}_{1,1}, \quad \Gamma_{2,0} = Z(\mathring{\Gamma}_{2,0} + 2K \mathring{\Gamma}_{1,1}), \tag{B15}$$

$$\Gamma_{1,2} = Z^{3/2} \mathring{\Gamma}_{1,2}, \quad \Gamma_{2,1} = Z^{3/2}(\mathring{\Gamma}_{2,1} + 2K \mathring{\Gamma}_{1,2}), \tag{B16}$$

$$\Gamma_{3,0} = Z^{3/2}(\mathring{\Gamma}_{3,0} + 3K \mathring{\Gamma}_{2,1} + 3K^2 \mathring{\Gamma}_{1,2}). \tag{B17}$$

Further exploiting the renormalization scheme (3.1) and using the scaling-invariant coupling constants $u = u_2 u_2'$, $v = u_1 u_2$, $w = u_0 u_2^3$, it requires only simple algebra to find

$$Z = 1 + \frac{u + 4v}{6\varepsilon}, \quad K = \frac{w - 2uv - 3v^2}{6u_2^2}, \tag{B18}$$

$$\underline{\underline{Z}} = \underline{\underline{1}} + \frac{1}{\varepsilon} \begin{pmatrix} 2u + 4v, & 5(w - 2uv - 3v^2)/3u_2^2 \\ -u_2^2, & u + 4v \end{pmatrix}, \tag{B19}$$

$$\underline{\underline{A}} = \frac{1}{\varepsilon u_2} \begin{pmatrix} 0, & u_2^2 \\ u_2^2, & -2v \end{pmatrix}, \tag{B20}$$

$$B_0 = \frac{11uw + 22vw - 10u^2 v - 29uv^2 - 22v^3}{2\varepsilon} u_2^{-3}, \tag{B21}$$

$$B_1 = \frac{16uv + 39v^2 - 5w}{6\varepsilon} u_2^{-1}, \tag{B22}$$

$$B_2 = \frac{2u + 6v}{\varepsilon} u_2 = (Z_2 - 1)u_2 \tag{B23}$$

for the one-loop renormalizations.

APPENDIX C: TWO-LOOP RESULTS OF THE RG FUNCTIONS

Here we list our two-loop results for the RG functions that went into the calculation of the critical exponents for the θ transition. Details of the calculation leading to these results will be presented elsewhere [37].

The two-loop parts of the α matrix are given by

$$\alpha_{1,1}^{(2)} = 1, \tag{C1}$$

$$\alpha_{1,2}^{(2)} = -\left(\frac{47}{24}u + \frac{35}{6}v\right), \tag{C2}$$

$$\alpha_{2,2}^{(2)} = \left(\frac{23}{4}u + \frac{161}{12}v\right)v - \frac{23}{12}w. \tag{C3}$$

The two-loop parts of the γ and γ' function read

$$\gamma^{(2)} = \left(\tfrac{37}{216}u^2 + \frac{7}{6}uv + \frac{191}{108}v^2\right) - \frac{13}{108}w, \tag{C4}$$

$$\gamma'^{(2)} = \left(\frac{29}{72}u + \frac{25}{27}v\right)w - \left(\frac{7}{12}u^2 + \frac{469}{216}uv + \frac{17}{9}v^2\right)v. \tag{C5}$$

The parts of the κ matrix that are not given by the shift invariance are

$$\kappa_{1,1}^{(2)} = \frac{611}{108}w - \left(\frac{1519}{108}u^2 + \frac{1403}{18}uv + \frac{10873}{108}v^2\right), \tag{C6}$$

$$\kappa_{2,1}^{(2)} = \left(\frac{43}{3}u^2 + \frac{3001}{54}uv + \frac{452}{9}v^2\right)v - \left(\frac{161}{18}u + \frac{580}{27}v\right)w. \tag{C7}$$

The β function that is not given by shift invariance reads

$$\beta_w^{(2)} = \left(\frac{55}{2}u^3 + \frac{10727}{72}u^2 v + \frac{4657}{18}uv^2 + \frac{887}{6}v^3\right)v - \left(\frac{2809}{72}u^2 + \frac{1754}{9}uv + \frac{1391}{6}v^2 - \frac{85}{9}w\right)w. \tag{C8}$$

[1] T. C. Lubensky and J. Isaacson, Phys. Rev. Lett. **41**, 829 (1978); **42**, 410(E) (1978); **20**, 2130 (1979).
[2] J. Isaacson and T. C. Lubensky, J. Phys. Lett. **41**, L469 (1980).
[3] A. B. Harris and T. C. Lubensky, Phys. Rev. B **23**, 3591 (1981); **24**, 2656 (1981).
[4] G. Parisi and N. Sourlas, Phys. Rev. Lett. **46**, 871 (1981).
[5] Y. Shapir, Phys. Rev. A **28**, 1893 (1983).
[6] P. G. deGennes, Biopolymers **6**, 715 (1968).
[7] R. Bundschuh and T. Hwa, Phys. Rev. Lett. **83**, 1479 (1999); Phys. Rev. E **65**, 031903 (2002); R. Bundschuh and T. Bruinsma, Phys. Rev. Lett. **100**, 148101 (2008).
[8] H.-P. Hsu and P. Grassberger, J. Stat. Mech. (**2005**) P06003.
[9] H.-P. Hsu, W. Nadler, and P. Grassberger, J. Phys. A: Math. Gen. **38**, 775 (2005).
[10] B. Derrida and H. J. Herrmann, J. Physique **44**, 1365 (1983).
[11] M. Henkel and F. Seno, Phys. Rev. E **53**, 3662 (1996).
[12] F. Seno and C. Vanderzande, J. Phys. A: Math. Gen. **27** 5813, 7937 (1994).

[13] S. Flesia, D. S. Gaunt, C. E. Soteros, and S. G. Whittington, J. Phys. A: Math. Gen. **25**, L1169 (1992); **27**, 5831 (1994).
[14] E. J. Janse van Rensburg *et al*., J. Phys. A: Math. Gen. **30**, 8035 (1997); **32**, 1567 (1999); **33**, 3653 (2000).
[15] A. Coniglio, J. Phys. A: Math. Gen. **16**, L187 (1983).
[16] F. Family and A. Coniglio, J. Phys. A: Math. Gen. **13**, L403 (1980).
[17] H. K. Janssen and A. Lyssy, J. Phys. A: Math. Gen. **25**, L679 (1992); Europhys. Lett. **29**, 25 (1995).
[18] H. K. Janssen and A. Lyssy, Phys. Rev. E **50**, 3784 (1994).
[19] J. Cardy, J. Phys. A: Math. Gen. **34**, L665 (2001).
[20] D. C. Brydges and J. Z. Imbrie, Ann. Math. **158**, 1019 (2003); J. Stat. Phys. **110**, 503 (2003).
[21] For a very clear pedagogically presentation of the work of Brydges and Imry see J. Cardy, e-print arXiv:cond-mat/0302495v3.
[22] H. K. Janssen and O. Stenull, Europhys. Lett. **90**, 46003 (2010).
[23] H. K. Janssen, M. Műller, and O. Stenull, Phys. Rev. E **70**, 026114 (2004).
[24] D. Stauffer and A. Aharony, *Introduction to Percolation Theory* (Taylor and Francis, London, 1994).
[25] C. Becchi, A. Rouet, and R. Stora, Commun. Math. Phys. **42**, 127 (1975).
[26] D. J. Amit, *Field Theory, the Renormalization Group, and Critical Phenomena* (World Scientific, Singapore, 1984).
[27] J. Zinn-Justin, *Quantum Field Theory and Critical Phenomena*, 4th ed. (Clarendon, Oxford, 2002).
[28] H. K. Janssen and U. C. Täuber, Ann. Phys. **315**, 147 (2005).
[29] H. K. Janssen, F. Wevelsiep, and O. Stenull, Phys. Rev. E **80**, 041809 (2009).
[30] For a recent review on the coherent path-integral approach see U. C. Täuber, M. Howard, and B. P. Vollmayr-Lee, J. Phys. A **38**, R79 (2005).
[31] H. K. Janssen, Z. Phys. **58**, 311 (1985).
[32] For a review, see e.g., L. Schäfer, *Excluded Volume Effects in Polymer Solutions* (Springer-Verlag, Berlin, 1999).
[33] H. K. Janssen, Z. Phys. B **23**, 377 (1976); R. Bausch, H. K. Janssen, and H. Wagner, *ibid*. **24**, 113 (1976).
[34] C. De Dominicis, J. Phys. C **37**, 247 (1976); C. DeDominicis and L. Peliti, Phys. Rev. B **18**, 353 (1978).
[35] H. K. Janssen, in *Dynamical Critical Phenomena and Related Topics*, edited by C. P. Enz, Lecture Notes in Physics, Vol. 104, (Springer, Heidelberg, 1979), p. 26; H. K. Janssen, in *From Phase Transition to Chaos*, edited by G. Györgyi, I. Kondor, L. Sasvári, and T. Tél (World Scientific, Singapore, 1992), p. 68.
[36] H. K. Janssen, J. Phys. C: Cond. Mat. **17**, S1973 (2005).
[37] H. K. Janssen and O. Stenull (in preparation).
[38] H. K. Janssen and O. Stenull (in preparation).
[39] J. des Cloizeaux, Phys. Rev. A **10**, 1665 (1974).
[40] M. E. Fisher, J. Chem. Phys. **44**, 616 (1966).
[41] D. McKenzie and M. Moore, J. Phys. A: Math. Gen. **4**, L82 (1971).